Cy.6

THE AEDC THREE-DIMENSIONAL, POTENTIAL FLOW COMPUTER PROGRAM

VOLUME II. MATHEMATICAL MODELING, APPLICATION, AND VERIFICATION

R.L. Palko

PROPULSION WIND TUNNEL FACILITY
ARNOLD ENGINEERING DEVELOPMENT CENTER
AIR FORCE SYSTEMS COMMAND
ARNOLD AIR FORCE STATION, TENNESSEE 37389

February 1976

Final Report for Period November 1971 — November 1974

Prepared for

DIRECTORATE OF TECHNOLOGY
ARNOLD ENGINEERING DEVELOPMENT CENTER
ARNOLD AIR FORCE STATION, TENNESSEE 37389

NOTICES

When U. S. Government drawings specifications, or other data are used for any purpose other than a definitely related Government procurement operation, the Government thereby incurs no responsibility nor any obligation whatsoever, and the fact that the Government may have formulated, furnished, or in any way supplied the said drawings, specifications, or other data, is not to be regarded by implication or otherwise, or in any manner licensing the holder or any other person or corporation, or conveying any rights or permission to manufacture, use, or sell any patented invention that may in any way be related thereto.

Qualified users may obtain copies of this report from the Defense Documentation Center.

References to named commercial products in this report are not to be considered in any sense as an endorsement of the product by the United States Air Force or the Government.

This report has been reviewed by the Information Office (OI) and is releasable to the National Technical Information Service (NTIS). At NTIS, it will be available to the general public, including foreign nations.
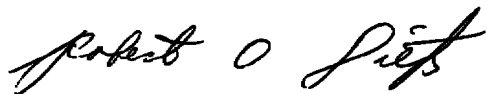
APPROVAL STATEMENT

This technical report has been reviewed and is approved for publication.

FOR THE COMMANDER

CARLOS TIRRES
Captain, USAF
Research & Development
 Division
Directorate of Technology

ROBERT O. DIETZ
Director of Technology

UNCLASSIFIED

REPORT DOCUMENTATION PAGE		READ INSTRUCTIONS BEFORE COMPLETING FORM
1 REPORT NUMBER AEDC-TR-75-75 Volume II	2 GOVT ACCESSION NO.	3 RECIPIENT'S CATALOG NUMBER
4 TITLE (and Subtitle) THE AEDC THREE-DIMENSIONAL, POTENTIAL FLOW COMPUTER PROGRAM - VOLUME II. MATHEMATICAL MODELING, APPLICATION, AND VERIFICATION		5 TYPE OF REPORT & PERIOD COVERED Final Report - November 1971 - November 1974
		6 PERFORMING ORG. REPORT NUMBER
7 AUTHOR(s) Richard L. Palko - ARO, Inc.		8 CONTRACT OR GRANT NUMBER(s)
9 PERFORMING ORGANIZATION NAME AND ADDRESS Arnold Engineering Development Center (DY) Air Force Systems Command Arnold Air Force Station, Tennessee 37389		10. PROGRAM ELEMENT, PROJECT, TASK AREA & WORK UNIT NUMBERS Program Element 65807F
11 CONTROLLING OFFICE NAME AND ADDRESS Arnold Engineering Development Center (DYFS) Air Force Systems Command Arnold Air Force Station, Tennessee 37389		12 REPORT DATE February 1976
		13 NUMBER OF PAGES 53
14 MONITORING AGENCY NAME & ADDRESS(if different from Controlling Office)		15 SECURITY CLASS. (of this report) UNCLASSIFIED
		15a DECLASSIFICATION 'DOWNGRADING SCHEDULE N/A

16 DISTRIBUTION STATEMENT (of this Report)

Approved for public release; distribution unlimited.

17 DISTRIBUTION STATEMENT (of the abstract entered in Block 20, if different from Report)

18 SUPPLEMENTARY NOTES

Available in DDC

19 KEY WORDS (Continue on reverse side if necessary and identify by block number)

three-dimensional flow	mathematical models
flow fields	modeling techniques
subsonic flow	potential flow
computer program	vortex lattice
computer analysis	

20 ABSTRACT (Continue on reverse side if necessary and identify by block number)

A complete description of a computer analysis of the potential subsonic flow about complex three-dimensional bodies is presented. The linear, partial differential equation for the compressible velocity gradient is solved for cases where the local Mach number everywhere in the flow field is less than one. The compressible flow equation is transformed, using Goethert similarity parameter, into the equivalent incompressible form represented by Laplace's equation. The solution to the equation is accomplished by

DD FORM 1473 1 JAN 73 EDITION OF 1 NOV 65 IS OBSOLETE

UNCLASSIFIED

20. ABSTRACT (Continued)

representing the body (or model) by a finite number of elements
(or singularities). The singularities may be made up of either
vortices or sources. The two volumes included in the report give
the description of the computer program which is entitled the AEDC
Potential Flow Program (PFP) and the computer analysis of several
complex bodies. Volume I includes a theoretical development of
the equations that lead to the set that are programmed in the PFP.
A complete description of the computer program is given along with
sample input and output from the program. Volume II includes a
discussion concerning the modeling techniques that can be used to
represent a wide class of three-dimensional bodies and gives the
results of the flow field computed about these bodies using the
PFP. Comparisons of some of the theoretical results are made with
wind tunnel experimental data.

AFSC
Arnold AFS Tenn

PREFACE

CONTENTS

ILLUSTRATIONS

Figure | Page

1.0 INTRODUCTION

In January 1971, a research effort was undertaken in the Propulsion Wind Tunnel Facility (PWT) at the Arnold Engineering Development Center (AEDC) to develop a new test technique for testing full-scale inlet/engine systems at high angles of attack and yaw. The steps taken in developing the new techniques were: (1) to determine for a given aircraft configuration the flow field at the inlet, (2) to develop flow shaping devices which are capable of producing the desired flow, and (3) to verify the ability of the device by conducting flow survey tests in the wind tunnel. The success of such an approach obviously depends on the ability to correctly determine the flow field produced by the aircraft and the flow shaping devices. To correctly determine these flow fields required either experimental data from wind tunnel tests or predictions made by analytical procedures. Wind tunnel testing was considered to be both too costly and time consuming because a large number of models would need to be fabricated and tested before the correct flow simulations were obtained. Therefore, it was determined that an analytical method of predicting the flow fields for both the aircraft and the flow shaping devices was needed.

At that time, a three-dimensional potential flow program which used a vortex-lattice to describe the model was in use at AEDC for flow field calculations. A compressibility correction using Goethert's Rule had been incorporated into the program for use at high subsonic Mach numbers. However, this program was fixed to use only 99 horseshoe vortices which restricted its use to very simple models. Since models with considerable detail would be required for the pending flow field analyses, the program was rewritten and expanded to allow the flow field for very large models to be analyzed. The flow field calculations made with this program gave excellent agreement with wind tunnel data (Ref. 2) which ultimately resulted in the development of the testing technique desired. However, the program proved to be extremely slow. Whereas the solution for a model with 99 vortices could be obtained in approximately 30 min, the solution for a model with 570 vortices (the largest tried with this version of the program) took approximately 20 hr. This was considerably less time than required for fabrication and testing of a model; however, the time factor obviously restricted the use of the program. A second rewrite of the program eliminated some unused routines and arranged the program in a more efficient manner in the computer, resulting in only a slight reduction in time to obtain a solution. Therefore, a complete rewrite of the potential flow solution was undertaken which resulted in the present Potential Flow Program (PFP). With this program, the solution for a model with 1579 vortices was obtained in 16 hr on the old AEDC IBM-370-155 which should reduce to approximately 4 hr on the present AEDC IBM-370-165.

During the development of the PFP, considerable effort was spent on perfecting modeling techniques. Many problems and failures were encountered. Some were obvious;

whereas, others required considerable study. This volume is intended to help the user of this program avoid some of the problems and failures that have already been encountered with models that have been used during the program development and that have been analyzed since the program has become a standard tool in flow field analyses at AEDC.

2.0 BASIC DATA OBTAINED FROM THE PFP

The Potential Flow Program (PFP) in the existing form was developed primarily as a result of the need to make calculations of the flow field in the vicinity of aircraft fuselages (typically at locations where aircraft inlets might be located). This need arose because of the support the theoretical flow field calculations could lend to a research program carried out at AEDC to simulate the inlet flow fields in a wind tunnel test of full-scale inlet/engine systems (Refs. 1 and 2). Much of the computing capability that the PFP currently has was a result of these flow field calculations which had as their primary variables the flow angularity (upwash and sidewash) over a y-z plane. After the initial solution of the velocity field for a given model attitude and Mach number is obtained, the upwash and sidewash can be determined for any given point or over any grid desired. A new solution is required for each model attitude or Mach number. In addition to computing the upwash and sidewash, the PFP also computes the local Mach number, C_p, and flow streamlines. A computer plotting program has been written to supplement the PFP, and computer plots can be obtained for most of the above parameters. The standard views plotted are the x-y, x-z, y-z, and an isometric, with the option of a perspective view from any angle if desired. A streamline can be traced from any point in the stream either upstream or downstream (or both). A very important capability of the program is that of plotting the model prior to running the complete solution. This allows corrections to be made with only a slight loss of computer time.

3.0 VORTEX-ELEMENT AND SOURCE/SINK REPRESENTATION
OF AERODYNAMIC BODIES (MODELING)

Unlike the computer program which has resulted from an exact science, the preparation of the mathematical models to be used in the program has proved to be more of an art than a science. If the disturbances on the ground caused by an aircraft flying at 10,000-ft altitude are desired, the aircraft could be represented by a cube, and the results would probably be acceptable. However, if the flow passing over a wing and entering an inlet located behind the wing is desired, then a model with considerably more detail will be required. Much of the time spent during the development of the PFP has been spent developing modeling techniques to fit the various study requirements. Although most aircraft models and flow studies will have their own peculiarities, the most complicated configuration can be described by general modeling techniques.

3.1 GENERAL MODELING TECHNIQUES

The mathematical representation of an aerodynamic shape, for which the flow field computation is desired from the PFP, is normally made up of a series of loop or horseshoe vortices connected together by common sides as shown in Fig. 1. A control point is normally located at the center of each loop or horseshoe (see Section 3.3 of Volume I). The control point is the location where the magnitude and direction of the velocity vector is specified (typically normal to the plane of the loop and equal to zero if simulating a solid surface). For simplicity, the model can be divided up into sections or, to use the common term, wing parts for setting up the vortex grid. One word of caution that will be repeated later is: where two wing parts join together, care should be taken to ensure that the common coordinates are identical. The loop vortices are used to represent the majority of any model with the horseshoe vortices normally being used only at the trailing edge of a lifting surface or as a flow shield to force the flow in a selected direction. (This will be discussed in a later section.)

∕∕	– LONGITUDINAL RAY
\\	– LATERAL RAY (CIRCUMFERENTIAL RAY)
+	– CONTROL POINT LOCATION
↑	– DIRECTION OF VORTEX
NO.	– ENTER SEQUENCE PER CARD
LETTER	– CARD SEQUENCE
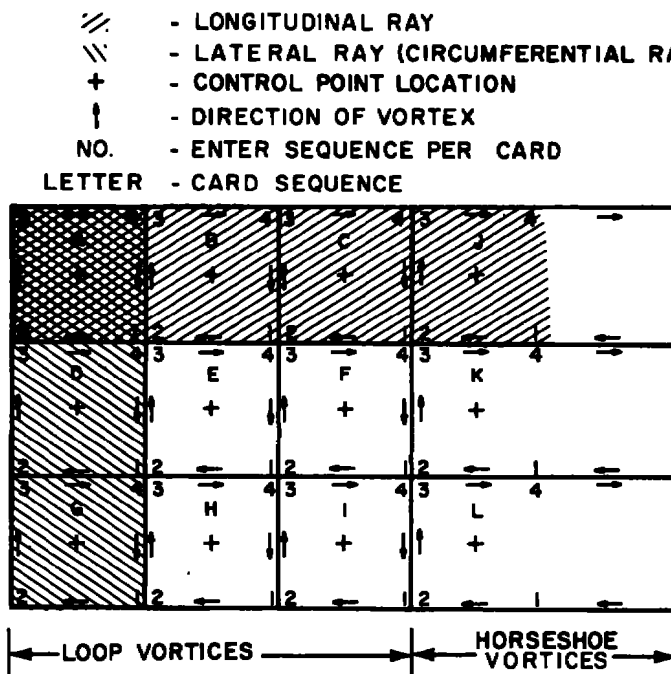
Figure 1. Typical wing part construction.

When setting up the vortex grid for a model never completely enclose the model with the grid network. For example, in modeling a cube, only five sides should be specified as shown in Fig. 2. If side 6 (the shaded side) is specified a singular matrix will result, and the program will stop. If horseshoe vortices are used with a model (again using a

① THRU ⑤ - LOOP VORTICES
⑥ - OPEN

②&③ - LOOP VORTICES
①,④&⑤ - HORSESHOE VORTICES
⑥ - OPEN
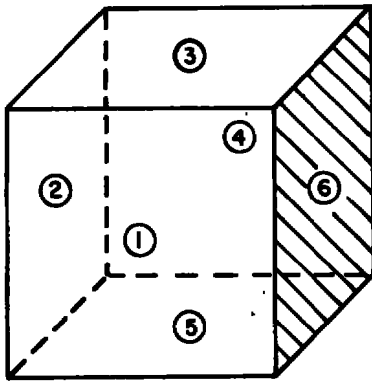
Figure 2. Cube mathematical model.
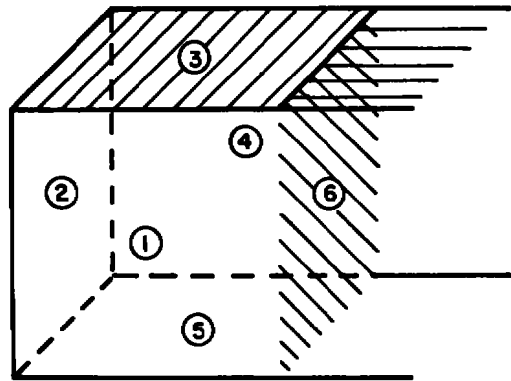
Figure 3. Cube mathematical model with trailing vortices.

cube for example) such as Fig. 3. only three of the sides adjacent to side 6 can have trailing vortices. Sides 1, 4, and 5 could be horseshoe vortices with side 3 a loop vortex. Side 2 would automatically be a loop vortex since it is opposite side 6. If side 3 is also a horseshoe vortex, then this again closes the system resulting in a singular matrix, and the program will stop.

For best results, the models should be constructed of square loop vortices, such as shown in Fig. 1, or at least rectangular loops that are uniform in both directions, such as shown in Fig. 4. However, most complicated models do not lend themselves to this type of pattern. Reference 3 suggests that, when a uniform grid is not practical, then at least a systematic variation should be used, such as spacing the vortex element in the direction necessary using the law of cosines, shown in Fig. 5. This should also apply to
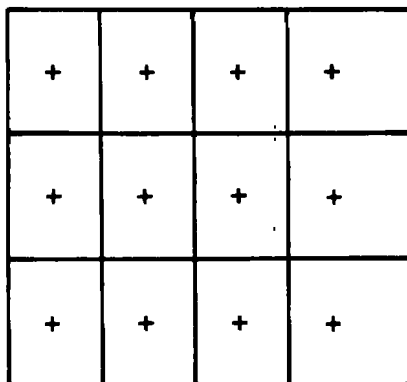
Figure 4. Wing part with rectangular construction.
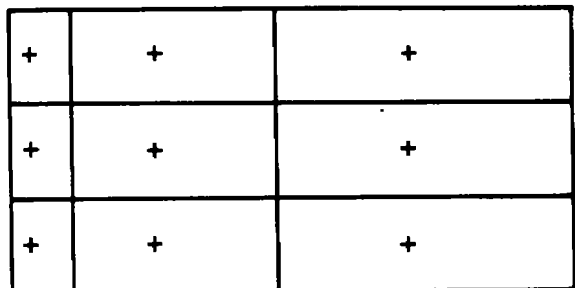
Figure 5. Wing part with law of cosine construction.

the location of the control points. The practice of using systematic variations has been followed to some extent although particular attention has not been given to trying to produce a cosine variation and the control points are usually located using the calculation routine in Vol. I (Section 3.3) in preparing the model input cards for the PFP program for convenience in modeling. If a different control point location is needed, it must be specified for each loop, and the calculation routine is not used. Although nonuniform spacing of vortex elements and control points causes some leakage in and out of the model, it is usually very local and self-compensating and, therefore, has become the standard modeling technique.

Each vortex loop used in the model increases the computer time required for a solution. This time increase is not linear but exponential. Therefore, effort should be placed on keeping the number of vortex loops to the minimum required for the accuracy needed. One way to achieve the optimum is to add new rays (the definition of rays is given in Fig. 1) to the model as needed and remove them when possible. Rays can be added either longitudinally, laterally, or both. This can be done using the "crows-foot" method in Fig. 6a. Experience has shown that the use of the direct addition method shown in
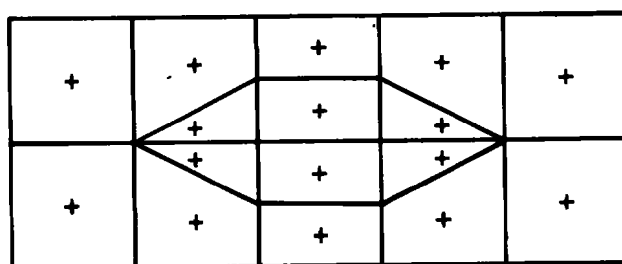
a. Correct
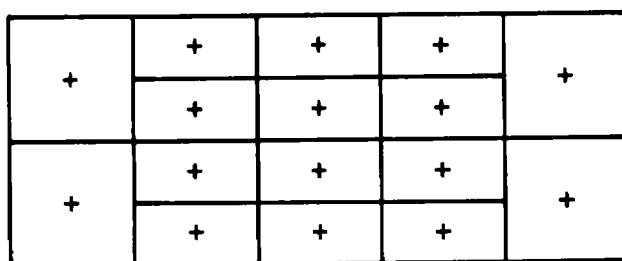
b. Incorrect

Figure 6. Addition and deletion of rays from wing parts.

Fig. 6b gives an incorrect simulation in the near flow field and should be avoided. A single ray can be added or removed if desired. To specify a triangular loop vortex for input into the program. it is still necessary to enter coordinates for four points on the input card. To do this, the coordinates for inputs 2 and 3 are entered with the identical

coordinates as shown in Fig. 7. A small segment of an actual model is shown in Fig. 8. Notice the location of the control points as placed by the computer program indicated by the "+" signs. There was, no doubt, some leakage in this area of the model with the control points located by the computer; a better location is shown with the circle. However, no significant effect on the flow field was indicated by such modeling techniques. The actual positioning for control points to produce no leakage in an area could be the subject of a study in itself.
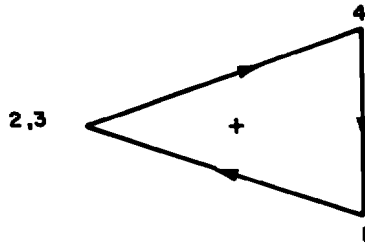
Figure 7. Triangular loop vortex.

+ CONTROL POINT, COMPUTER LOCATION
O CONTROL POINT, BETTER LOCATION
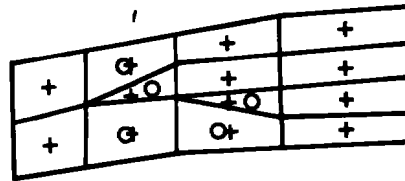
Figure 8. Typical wing part construction for complex model.

A special feature of the PFP that results in considerable savings of computer time involves the use of symmetry (Section 3.2 of Vol. I). If the model is symmetrical about the plane in which the free-stream velocity vector lies (see Fig. 9), only one-half of the model has to be input into the program, and the program uses not only the inputs but all of their reflections. If the model is symmetrical about two planes in which the free-stream velocity vector lies, only one-quarter of the model has to be input into the program.
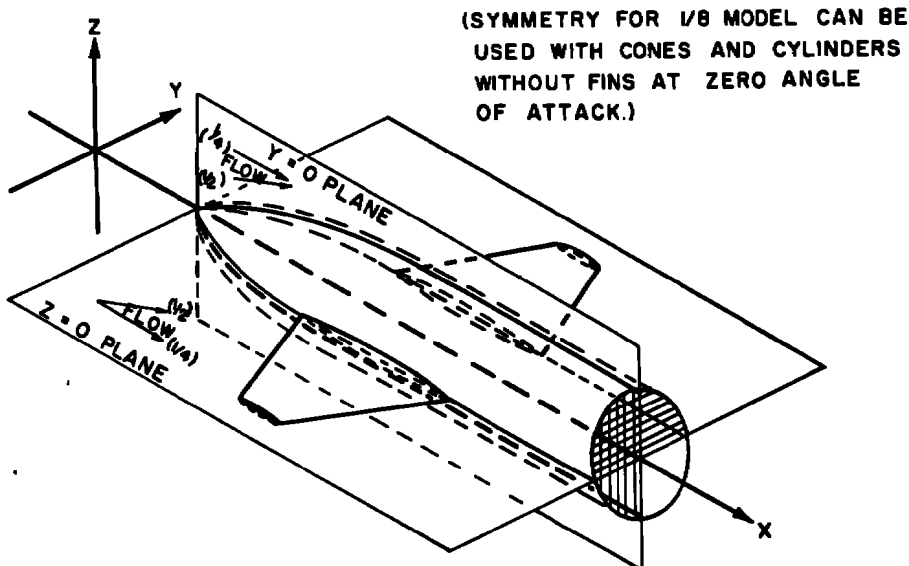
Figure 9. Model with various planes of symmetry.

In setting up the vortex grid for a model, the rays are generally set closer together perpendicular to the free stream for best results. The spacing of the rays determines the minimum distance from the model surface for which an accurate value of the flow velocity can be computed. The effect of different spacing of both sets of rays is shown clearly in Figs. 10 and 11. Figure 10 gives a computed streamline around a 10-deg cone with three different vortex grid spacings. Symmetry was used with only one-half the cone modeled. In Fig. 10a, the 1/2-cone was divided into five rays circumferentially (laterally) and four rays longitudinally. The open symbol indicates a distance from the cone equal to the space between circumferential vortices, and the solid symbol indicates a distance from the cone equal to the space between longitudinal vortices. Three streamlines were traced. The two streamlines nearest the cone wrapped around one of the circumferential vortices. The third streamline went over the model but shows a slight local influence of each longitudinal vortex. If data at any of these spacings were needed, this model would not be adequate. In Fig. 10b, rays were added between each ray circumferentially. The results were identical to those shown in Fig. 10a. In Fig. 10c, the rays are added between each longitudinal ray. Here the outside two streamlines were good, whereas the inside streamline shows a local influence at each circumferential vortex. Note that the inside streamline passes just inside the solid symbol, which denoted a distance from the model equal to the spacing between longitudinal vortices.

Figure 11 shows a similar analysis of a cylinder in a cross flow. In Fig. 11a, the cylinder was divided into four rays circumferentially and seven rays longitudinally. Again the open and solid symbols indicate the distance from the model. Note that the inside streamline wrapped around one of the circumferential vortices and the other two streamlines both show local influence at each circumferential vortex. Also notice that all three of the streamlines are nearer the model than either symbol. In Fig. 11b, a ray was added between each of the longitudinal rays. Again the results were identical to those shown in Fig. 11a. In Fig. 11c, the rays were added between the circumferential rays. Notice that all three streamlines are now smooth and that the inside streamline passes directly over the open symbol.

A good rule-of-thumb indicated by Figs. 10 and 11 is that the PFP will compute accurate flow velocities up to a distance from the model surface equal to the spacing between the vortices that run perpendicular to the free stream.

13

○ CIRCUMFERENTIAL SPACING DISTANCE ABOVE MODEL

● LONGITUDINAL SPACING DISTANCE ABOVE MODEL
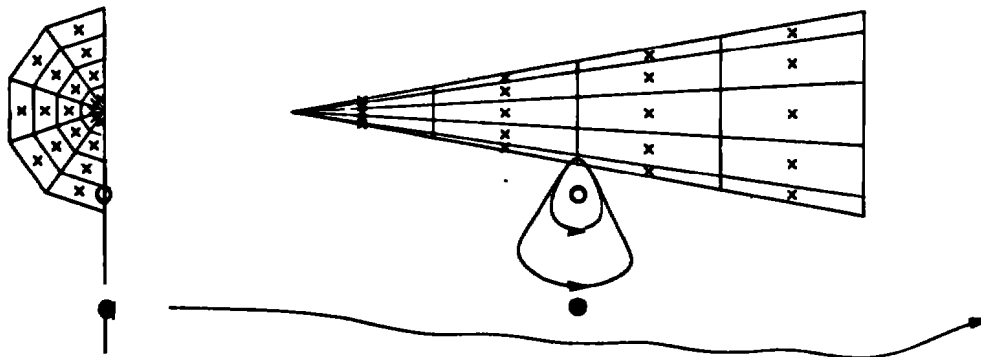
a. Base configuration
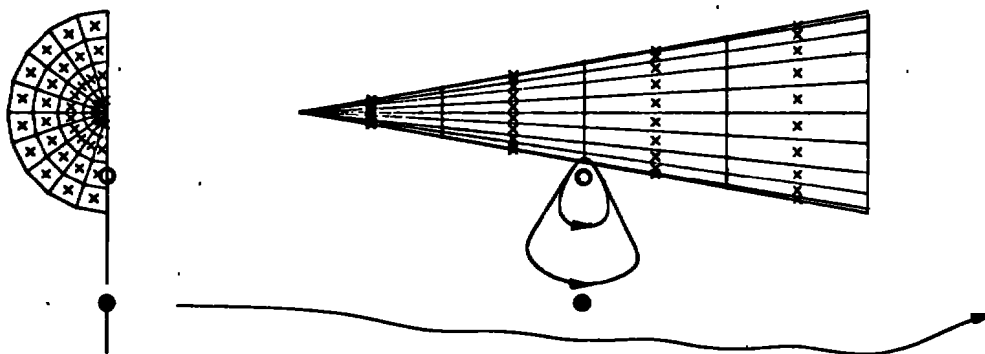
b. Configuration with close circumferential spacing
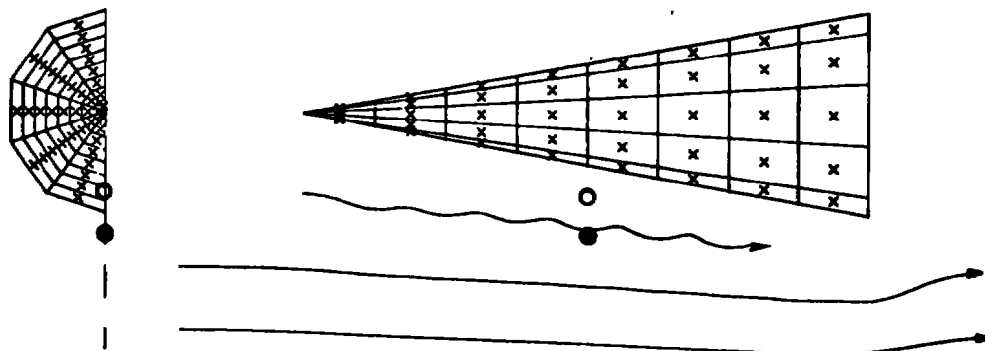
c. Configuration with close longitudinal spacing
Figure 10. Flow analysis for 10-deg cone.

14

○   CIRCUMFERENTIAL SPACING DISTANCE ABOVE MODEL
●   LONGITUDINAL SPACING DISTANCE ABOVE MODEL
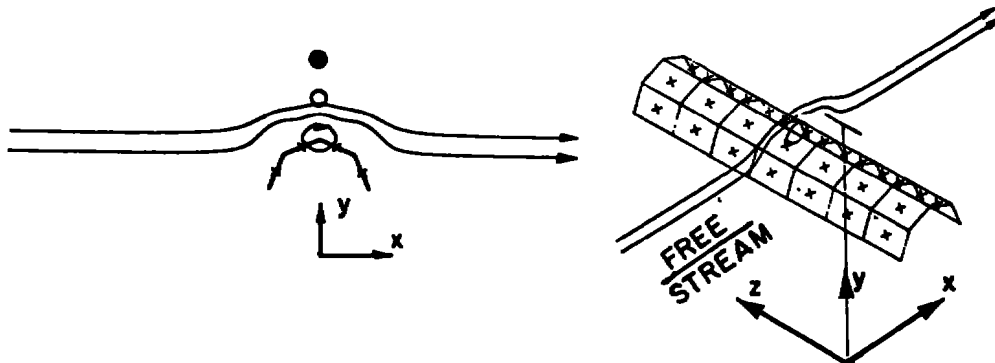
a. Base configuration
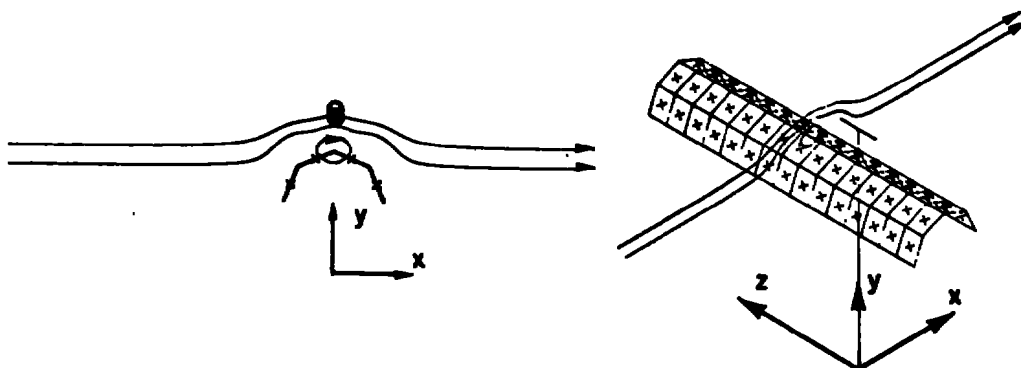
b. Configuration with close longitudinal spacing
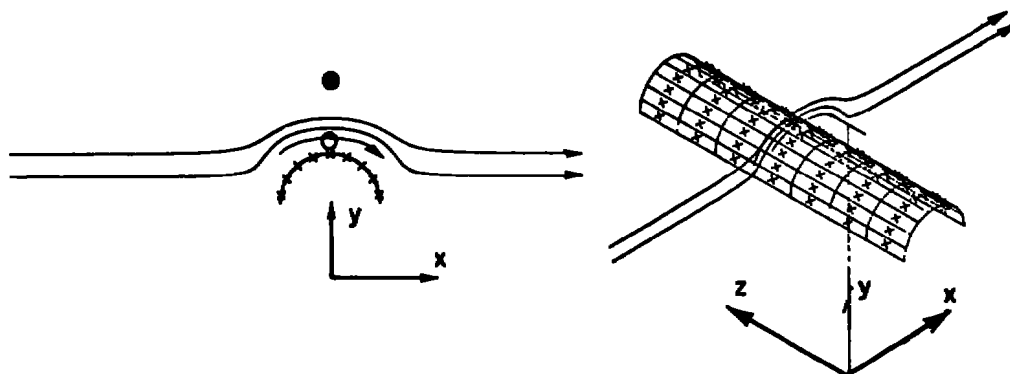
c. Configuration with close circumferential spacing
Figure 11. Flow analysis for cylinder in cross flow.

If a cone-cylinder body is to be analyzed from 0- to 90-deg angle of attack, then the technique of both Figs. 10 and 11 applies. This would be a case where the "crows-foot" modeling technique should be applied. The model in Fig. 12a would give satisfactory results at low angles of attack but poor results at high angles of attack. This model has 32 loop vortices in the cone. If rays are added to satisfy the cylinder requirements at high angles of attack (Fig. 12b). the cone ends up with 64 loop vortices with a circumferential spacing that is much closer than needed. However. if the "crows-foot" technique is used (Fig. 12c), the resulting model will end up satisfying both the high and low angle of attack requirements with only 44 loop vortices in the cone with a more uniform spacing.
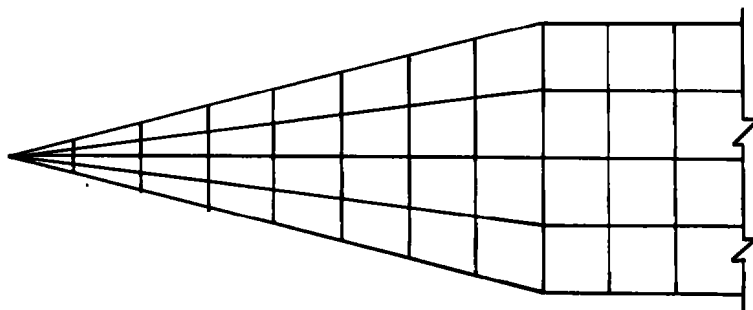
a. Cone with 32 loop vortices
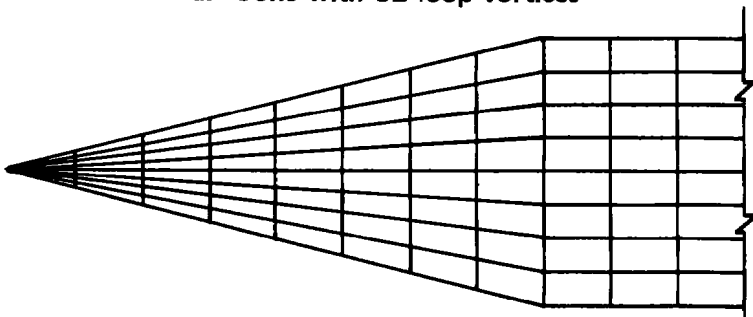
b. Cone with 64 loop vortices
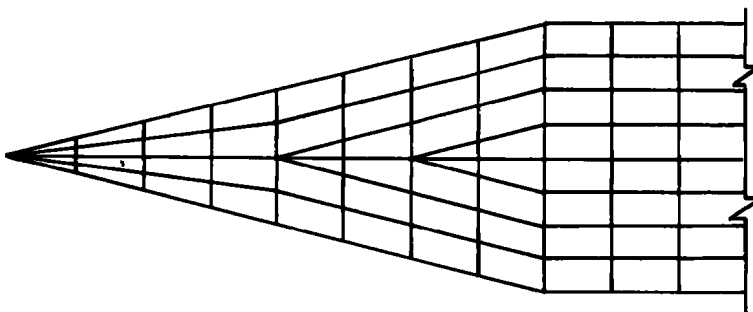
c. Cone with 44 loop vortices

Figure 12. Cone-cylinder mathematical model.

3.2 SPECIAL MODELING TECHNIQUES

3.2.1 Flow into Tubes and through Panels

For most model applications, the loop vortices are used to represent a solid surface by locating the control point at the center of the loop and specifying the normal velocity at the control point as zero. However, this is not a requirement of the PFP. Two special modeling techniques that can be used with the PFP involve flow through a tube and flow through loop vortices. These two techniques were used in Refs. 4 and 5. The analysis in these references was made with an earlier version of the PFP. However, the modeling techniques are the same, and since the modeling is described in detail in the cited references, only a brief description is given here.

A simple tube model is shown in Fig. 13 which might represent a fan-in-wing configuration. The requirement here is to have a specified mass flow into the tube, representing the fan jet, with trailing vortices without closing the system. To do this, an extra loop vortex is added to the end of the tube with only the coordinates common to the open-end coordinates of the horseshoe vortices. The control point for this extra loop is located at the entrance of the tube, and the velocity is specified to give the flow
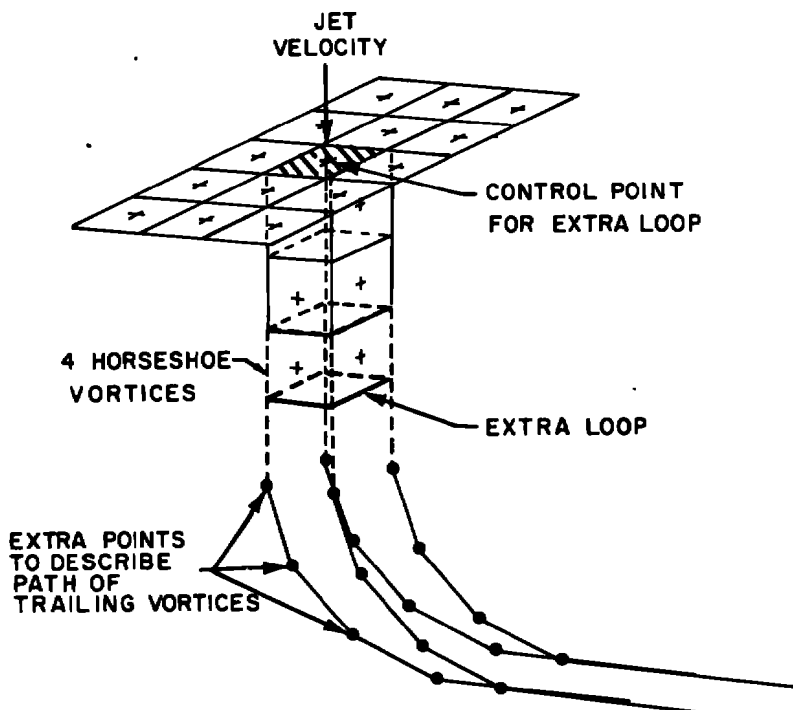
Figure 13. Fan-in-wing mathematical model.

velocity desired. If the loop vortex is put at the top of the tube with the normal control point location, the system is closed and the program will not give a solution. If it is necessary for the trailing vortices to follow a path other than a straight line as used in Refs. 4 and 5 (see Fig. 13), a small change is required in the PFP. This change would involve specifying the extra points along the path of the trailing vortices as a new type singularity (three types of singularities are specified in the program as written) and writing a subroutine to handle this new type singularity. This technique is available at AEDC as a special application but has been omitted from the general program.

+ CONTROL POINTS WITH NORMAL VELOCITY = 0
O CONTROL POINTS WITH NORMAL VELOCITY > 0
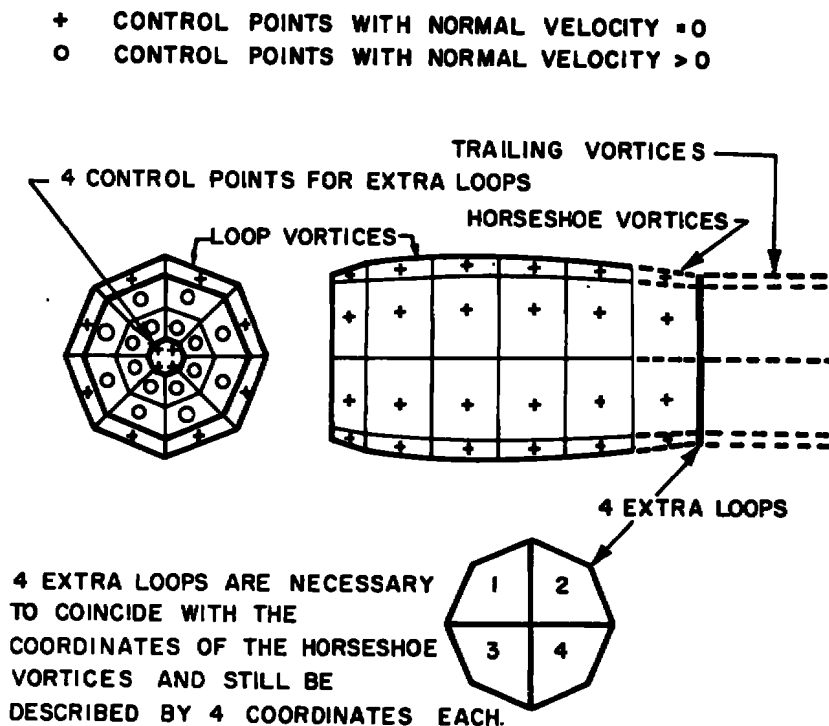
Figure 14. Variable power nacelle mathematical model.

A typical model that would require using controlled flow through some loop vortices is shown in Fig. 14. This model represents an engine nacelle with an exhaust jet. The nacelle is modeled with the usual loop vortices, except for the last circumferential ray, which are horseshoe vortices with the trailing vortices simulating the exhaust jet. The inlet of the nacelle is made up of 16 loop vortices for which the normal velocity component is specified to give the correct mass flow into the engine for the desired engine power setting. To keep from closing the system and still use the trailing vortices, four extra loop vortices are added at the exit of the nacelle similar to the extra loop vortex used in Fig. 13. The control points for these extra loops are located at the inlet in the opening which represents the fan hub. However, in this configuration, the normal velocity at the

control points for the extra loops is specified as zero. This model will work with the PFP as written. However, if the extra point singularity subroutine described in the previous paragraph is available, then only one extra horseshoe vortex is needed to replace the four extra loop vortices of Fig. 14 as shown in Fig. 15. With this method, the trailing vortices from the horseshoe are tied at a common point and trailed together resulting in a net strength of zero from that point.
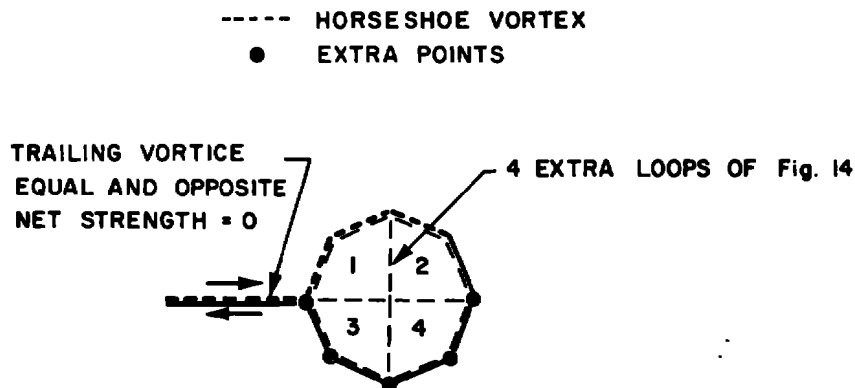
Figure 15. Horseshoe vortex with extra points.

3.2.2 Sources

One of the singularities that is available in the PFP is a point source. These point sources can either be positive or negative depending on whether flow is to be added to or removed from the system. An example where both positive and negative sources are used is shown in Fig. 16. This figure represents a wind tunnel with slotted top and bottom walls. The control points have been omitted from the sketch for clarity. For this representation the ends are closed and positive sources placed in the upstream end with equal negative sources placed at the downstream end. The source strengths are specified to give the desired mass flow velocity in the wind tunnel.

3.2.3 Airfoil Modeling

Several methods and special techniques have been applied at AEDC to model airfoils. The first method represented the model with a sheet of vortices. Considerable effort was applied to developing this technique with some of the results reported in Ref. 3, and the rules outlined in that reference have generally been followed when the primary interest is the lifting surface. This basic model technique is illustrated in Fig. 17. The airfoil mean line is represented with the vortex sheet with the vortices trailed at one-half of the angle between a line tangent to the mean line and the free-stream velocity vector. The loop vortices are set back from the leading edge a distance equal to one-quarter of the loop cord and set in from the tip a distance equal to one-quarter of the loop span.

19

● POSITIVE SOURCES
○ NEGATIVE SOURCES
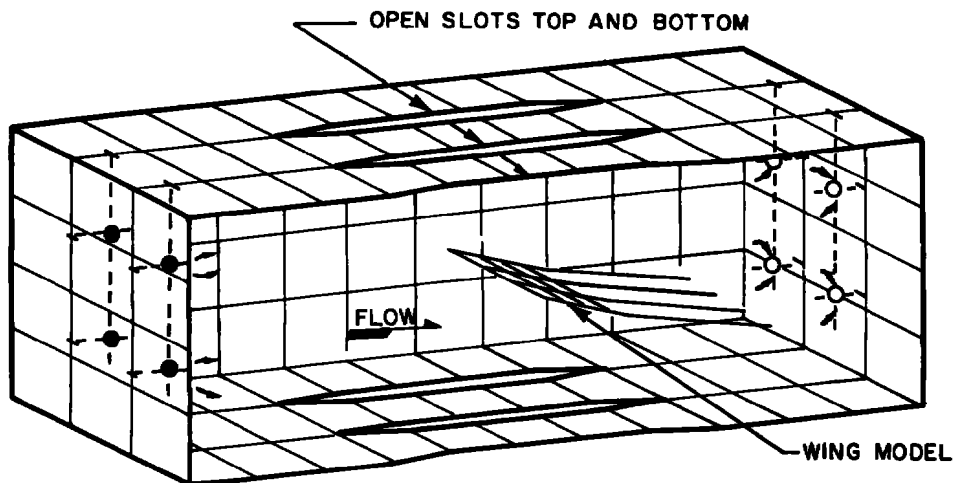
SYMMETRY ABOUT OPEN SIDE OF TUNNEL (PLANE y = 0)

Figure 16. Slotted wall wind tunnel mathematical model.
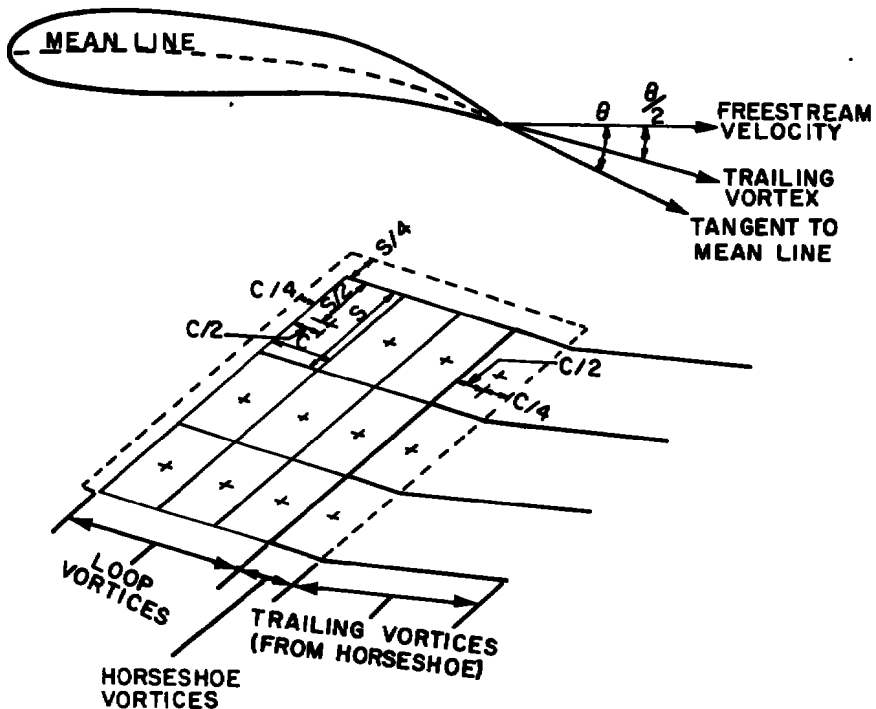
Figure 17. Lifting surface modeling technique.

20

TECHNIQUE 1

TECHNIQUE 2
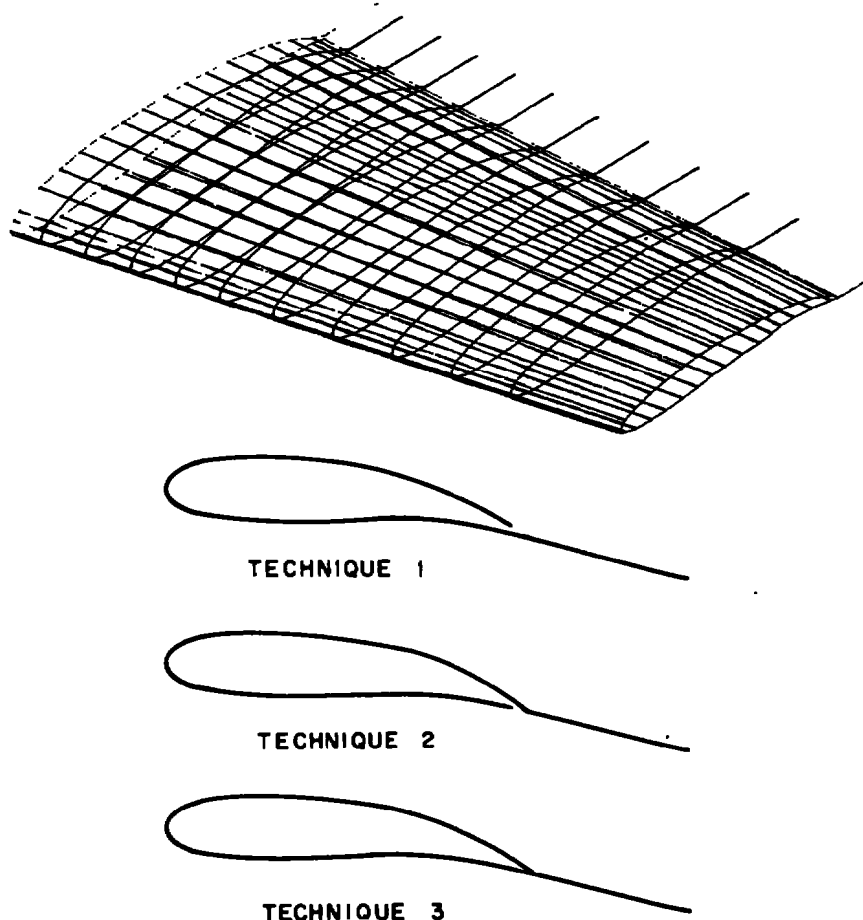
TECHNIQUE 3

Figure 18. Airfoil modeling technique.

When the primary interest was in the flow field near the airfoil or an area closely affected by the airfoil (which has usually been the case), then the entire surface of the airfoil has been modeled. Three techniques of modeling have been used as shown in Fig. 18. The difference in the three techniques is in the modeling of the trailing edge. Techniques 1 and 2 have been used most of the time. If the area of interest is under the airfoil, then Technique 1 (Fig. 18) is used. With this technique, the last lateral ray on the bottom is represented by horseshoe vortices with trails of the same angle indicated in Fig. 17. The rest of the surface is represented by loop vortices with a small gap (dependent on the chordwise vortex spacing) at the upper trailing edge. If the area of interest is above the airfoil, then Technique 2 (Fig. 18) is used. With this method the horseshoe vortices are on the top surface and the gap is on the bottom. These two techniques will work with the tip and root of the wing closed without closing the grid network. Excellent results have been obtained with both techniques.

Technique 3 (Fig. 18) can be used to obtain data both above and below the airfoil. With this technique, the last lateral ray on either the top or the bottom surface can be

horseshoe vortices, and no gap is left. The trailing edge coordinates for the last lateral ray of loop vortices are common with the trailing edge coordinates for the horseshoe vortices. With Technique 3, either the tip or root (or both) must be left open to keep from closing the system, which would result in causing the PFP not to give a solution.

A comparison of streamlines computed around a wing using Techniques 2 and 3 is shown in Fig. 19. In both cases, the wing was pitched 8 deg and the Mach number 0.3. The vortices were trailed at an angle of 11 deg. Both techniques gave good solutions. However, it appears that the vortex sheet was not trailed at exactly the correct angle, and the trailing edge gap of Technique 2 decreased the pumping effect of the sheet giving a better solution in this case.
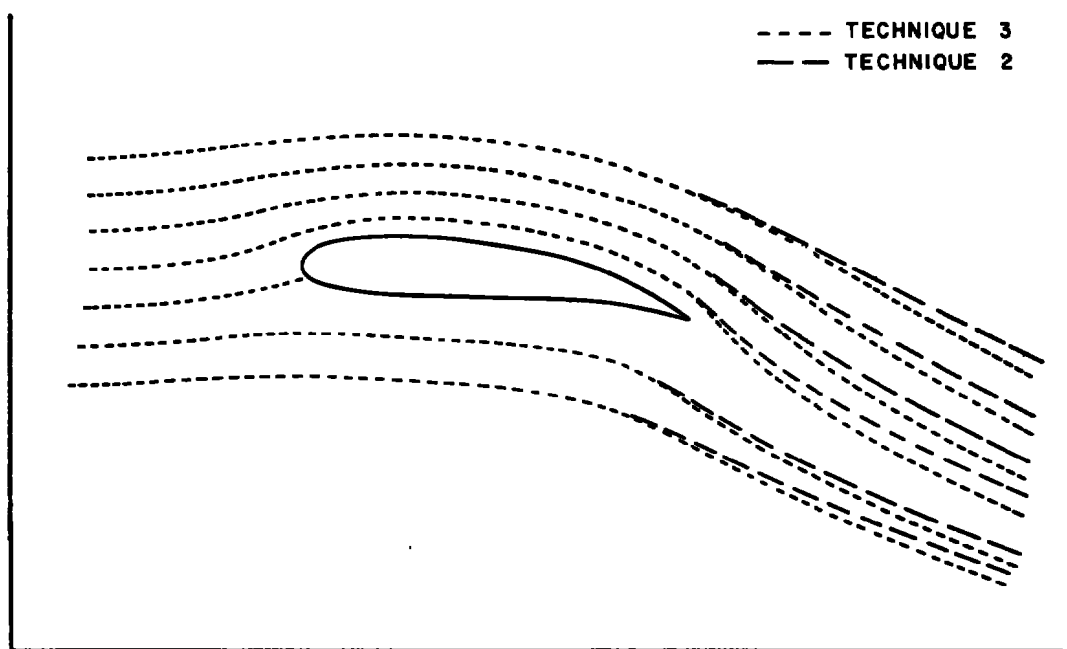
Figure 19. Comparison between airfoil modeling techniques
($M_\infty = 0.3$ and $a = 8$ deg).

For a thin airfoil, care must be taken in spacing the vortices and control points on each surface. An example of this modeling technique is shown in Fig. 20. If the vortices are spaced as in Case 1 (Fig. 20), the solution would be dominated by the lower surface vortices. In fact, it is doubtful if a difference would be detected if the top surface was left off. A better distribution is shown in Case 2 (Fig. 20) which would require approximately the same number of loop vortices. Here, the spacing is the same on the top and bottom surface and the control points are placed opposite each other. However, a still better distribution is shown in Case 3 (Fig. 20). Here the loop vortex cord has been set to no greater than four times the space between the top and bottom surface.

When a flattened fuselage with a thin wing is modeled and the area of interest is basically under (or over) the fuselage, the technique shown in Fig. 21 can be used. Here the fuselage-wing (Fig. 21a) can be modeled with the wing as a plane surface (Fig. 21b). The fuselage-wing junction can be set up like the example shown in Fig. 21c. This was the technique used to model the Fuselage-Wing model which will be described in Section 4.2.
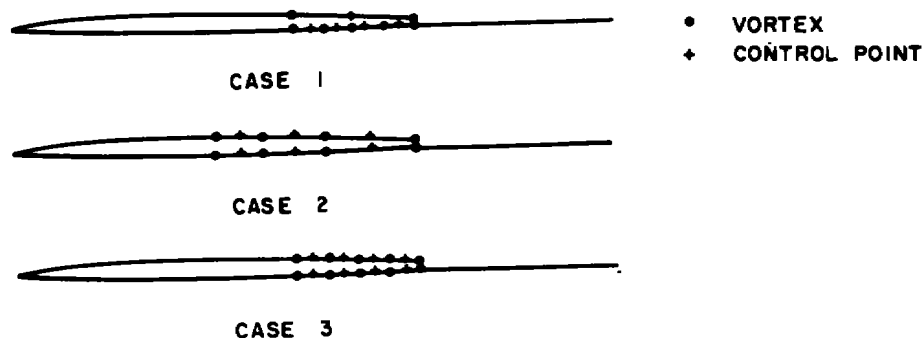
Figure 20. Thin wing modeling technique.

a. Fuselage-wing model

c. Fuselage-wing junction

b. Fuselage-wing simulation
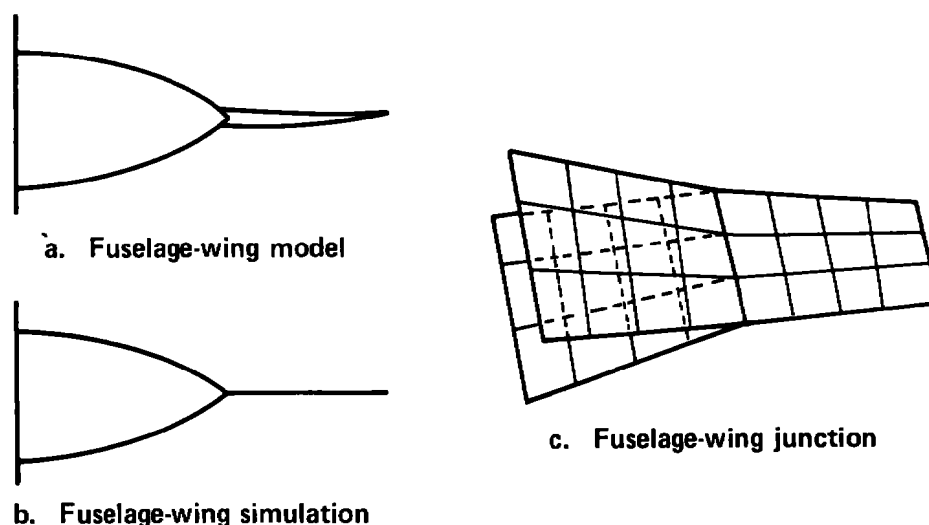
Figure 21. Fuselage-thin wing modeling.

3.2.4 Trailing Vortices as Flow Shield

Horseshoe vortices are usually used at the trailing edge of lifting surfaces; however, they have been used effectively as a flow shield to induce the flow around a body in a selected direction. Trailing vortices were used to simulate the jet roll up in Ref. 5.

One model used in this reference to simulate the jet from an isolated propeller in a cross flow is shown in Fig. 22. The objective of this type model is to force the flow around the trailing vortex shield to simulate the jet roll up. Details of how this modeling is done are shown in Fig. 23. This figure represents one circumferential ray of the jet tube shown in Fig. 22. Each ray has two horseshoe vortices and five loop vortices. The trailing horseshoe vortices are directed in a predetermined pattern with extra point singularities (see Section 3.2.1).

Directed Trailing
Vortices from
Horseshoes

Typical Horseshoe
(See Fig. 23)

Typical Loop
(See Fig. 23)
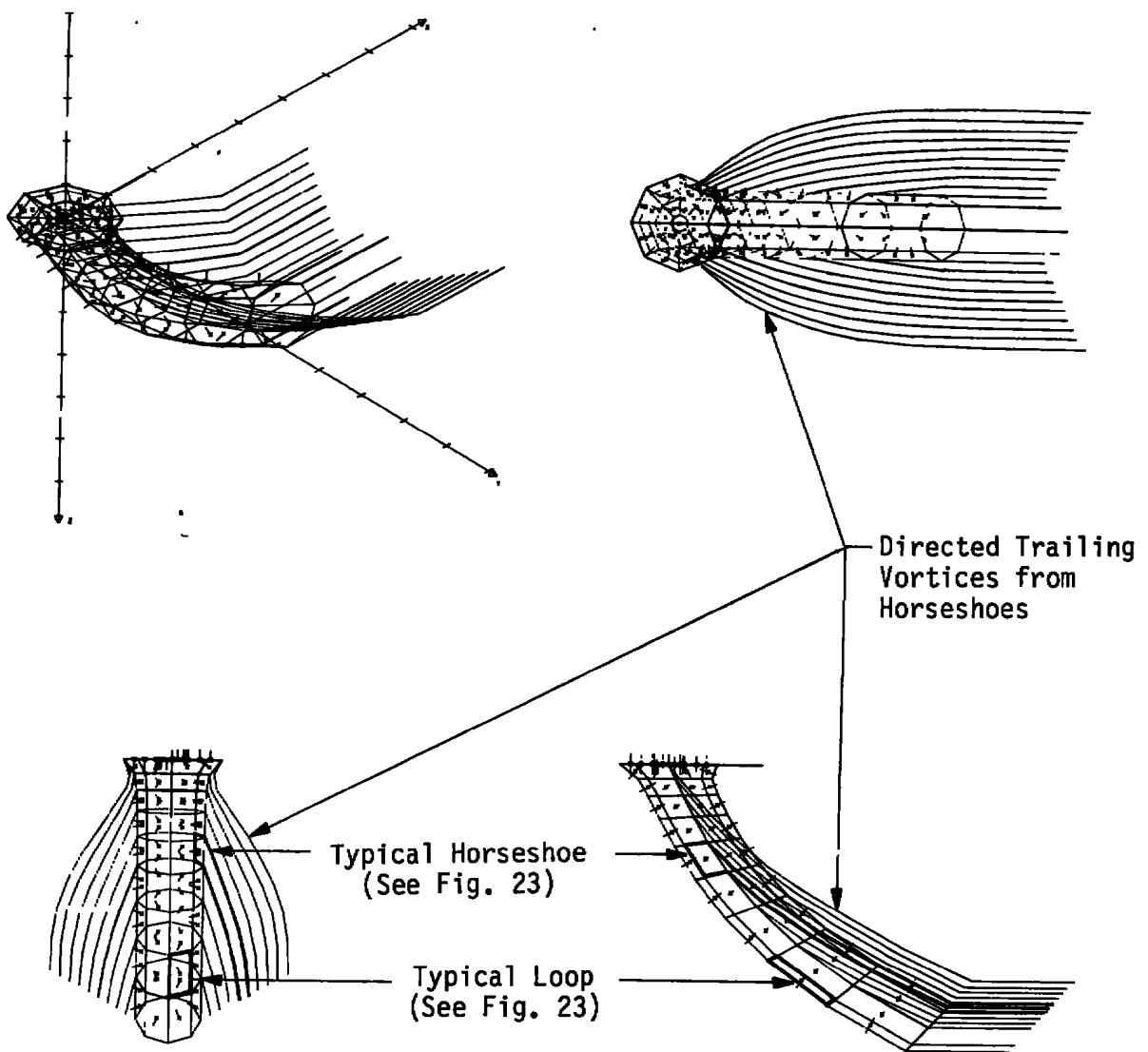
Figure 22. Mathematical model of free propeller in a crossflow.

HORSESHOE VORTICES
LOOP VORTICES
EXTRA POINT SINGULARITIES (SEE SECTION 3.2.I)

A SEGMENT OF JET MODEL
SHOWN IN Fig 22
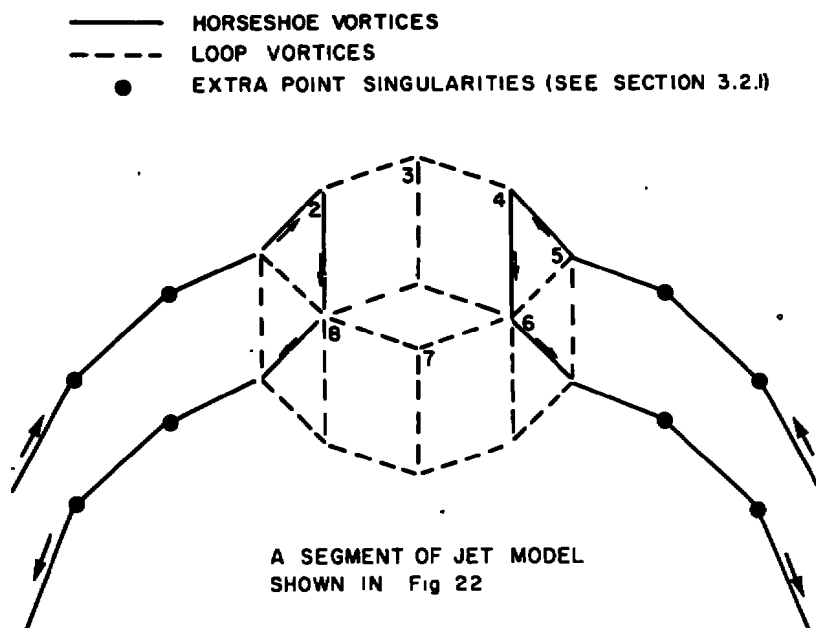
Figure 23. Circumferential ray of free propeller model.

3.3 MODEL LAYOUT TECHNIQUES

In the PFP, all mathematical modeling of the body in question must be done separately and input to the program in the format given in Section 3.3, Vol. 1, with coordinates for four points (corners of loop or horseshoe vortices) on each record. At AEDC, the model information is usually supplied to the computer programmer in a general form. The information given for a typical simple model such as a cone-cylinder is shown in Fig. 24. This figure gives the specifications for the model and the information needed. The programmer takes this information and writes some simple computer routines that determine the coordinates for the points on the cone and cylinder, organize the loops, and convert the coordinates to the alpha-type data sets needed for input in the PFP. The cards would normally be ordered circumferentially starting at the nose with the first circumferential ray input on cards 1 through 4, the second ray input on cards 5 through 8, etc., with the 12th ray input on cards 69 through 76. The coordinates for four points are required for each loop as shown with the inserts in Fig. 24 with only one loop per card. The coordinate system used in the program has been set up for "z" to be positive upward. If this system is not followed (it is not required), the scale must be specified in the plot program or the model will be plotted upside down. If this system is followed, the plot program will determine the scale based on the size of the model. After the model information is generated, the model is plotted and checked prior to running the computer program.

10° CONE + 2-in dia CYLINDER WITH SYMMETRY

CONE LENGTH = CYLINDER LENGTH

LONGITUDINAL SPACING
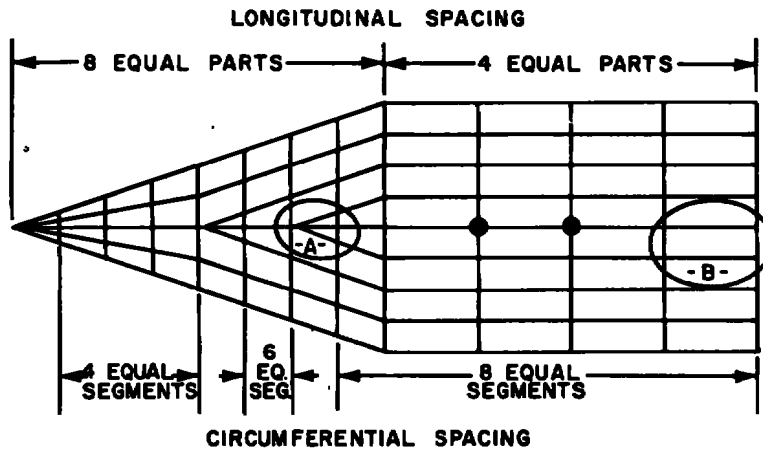
M∞ = 0.9, a = 45°

4 STREAMLINES- 2 EACH FOR 2 POINTS INDICATED AT DISTANCES
FROM THE SURFACE EQUAL TO THE LONGITUDINAL
AND CIRCUMFERENTIAL SPACING OF THE CYLINDER
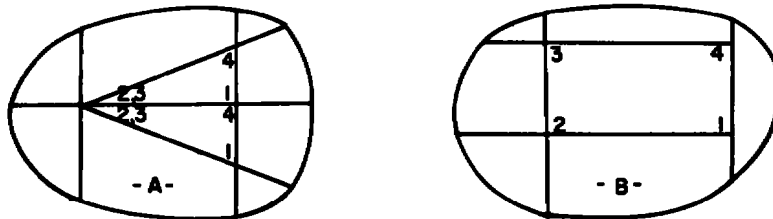
Figure 24. Typical engineers layout for simple model.

When modeling a complicated model, a complete tabulation of the coordinates of the vortex loops must be supplied to the programmer. Typically, a line drawing of the aircraft is available such as shown in Fig. 25. These drawings are usually drawn to a scale that will transfer to 1-in. graph paper with a readable scale. If this is the case, then the easiest method of modeling is to trace the cut lines of Fig. 25b on 1-in. graph paper with the buttlines on the corresponding station lines as shown in Fig. 26a. Then divide the cut lines circumferentially such that the spacing matches the accuracy required. Next connect the points from cut line to cut line in the most uniform manner possible as shown in Fig. 26a. If sufficient cut lines are not available, then some additional cuts can be added by extrapolation between the available fuselage cut lines. The y-z coordinates are then read directly from the graph paper for each point at each x-station and tabulated
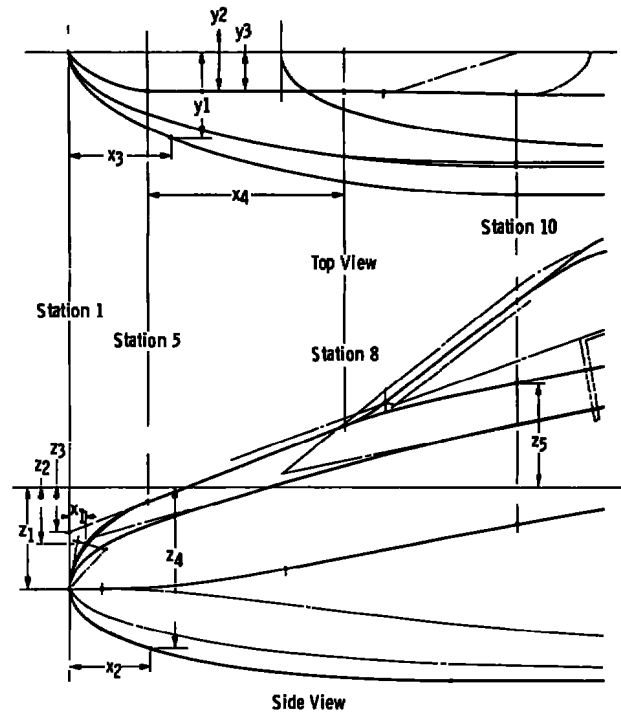
a. Model two view drawing
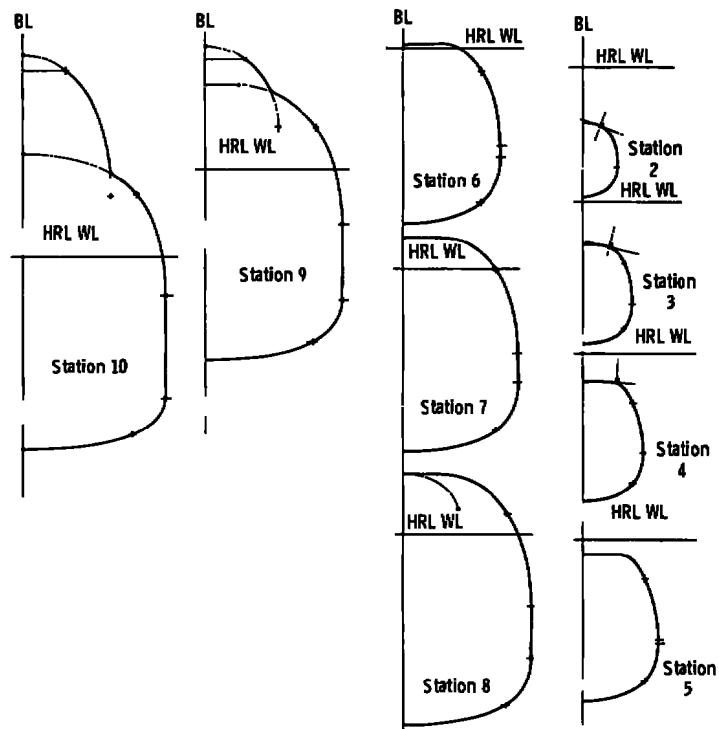
b. Fuselage section lines

Figure 25. Typical fuselage line drawings.

NOTE. ON THIS MODEL "Z" WAS POSITIVE UPWARDS
AND THE PLOT SCALES SPECIFIED

-A- SEE Fig 26b

REF W L

X-STA.—► I 2 3 4 5 6 7 8 9 10 11 12
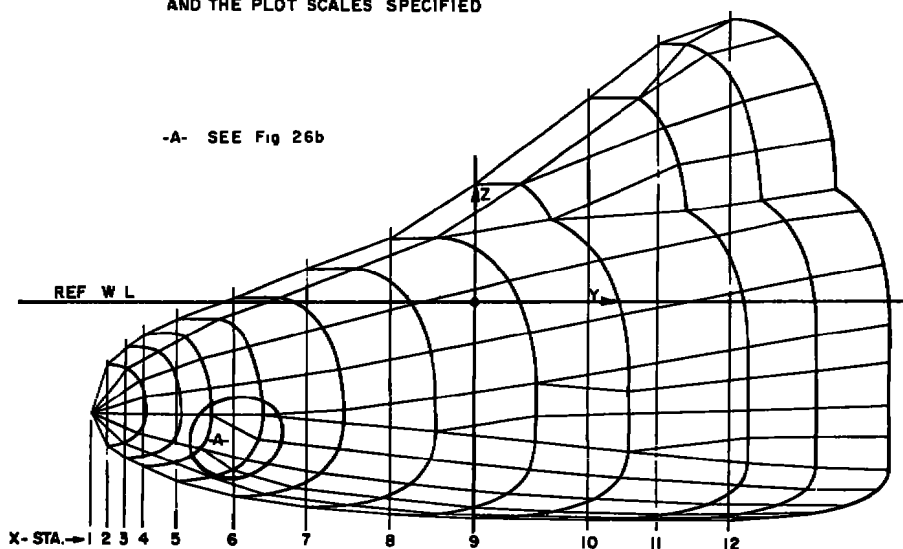
a. Line drawing layout
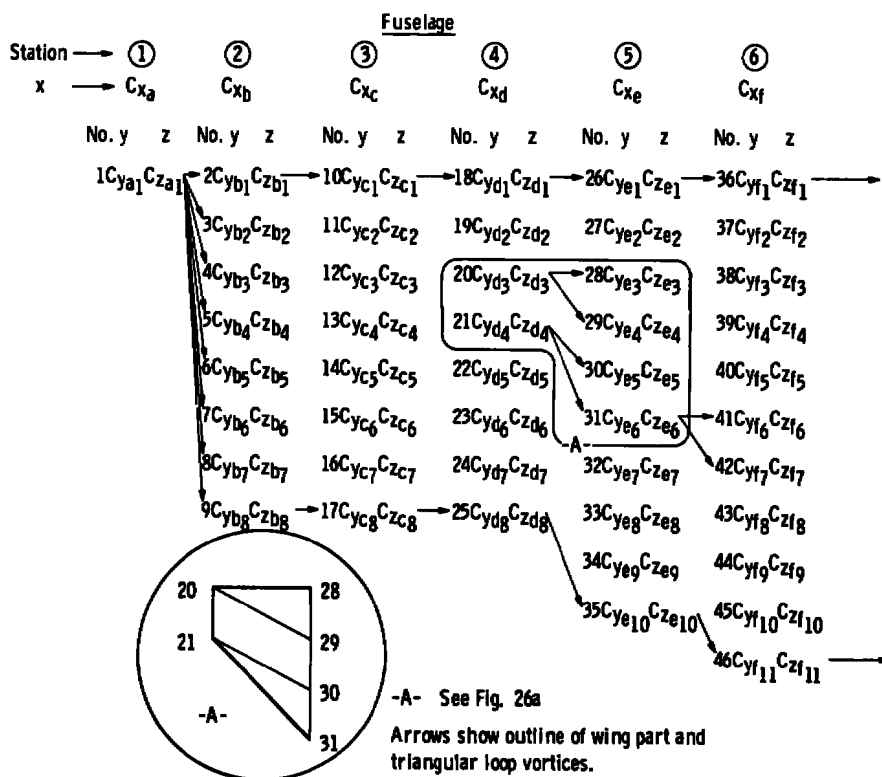
b. Coordinate tabulation

Figure 26. Fuselage layout for complex model.

No.	x	y	z
1	c_{x_a}	$c_{y_{a1}}$	$c_{z_{a1}}$
2	c_{x_b}	$c_{y_{b1}}$	$c_{z_{b1}}$
3	c_{x_b}	$c_{y_{b2}}$	$c_{z_{b2}}$
4	c_{x_b}	$c_{y_{b3}}$	$c_{z_{b3}}$
5	c_{x_b}	$c_{y_{b4}}$	$c_{z_{b4}}$
6	c_{x_b}	$c_{y_{b5}}$	$c_{z_{b5}}$
7	c_{x_b}	$c_{y_{b6}}$	$c_{z_{b6}}$
8	c_{x_b}	$c_{y_{b7}}$	$c_{z_{b7}}$
9	c_{x_b}	$c_{y_{b8}}$	$c_{z_{b8}}$
10	c_{x_c}	$c_{y_{c1}}$	$c_{z_{c1}}$
11	c_{x_c}	$c_{y_{c2}}$	$c_{z_{c2}}$
12	c_{x_c}	$c_{y_{c3}}$	$c_{z_{c3}}$
.	.	.	.
n	c_{x_n}	c_{y_n}	c_{z_n}

c. Coordinate listing

Loop I. D.				Singularity I. D.
1	2	3	1	2
1	3	4	1	2
1	4	5	1	2
.	.	.	.	.
1	8	9	1	2
2	10	11	3	2
3	11	12	4	.
.	.	.	.	.
8	16	17	9	.
.	.	.	.	
18	26	27	19	
19	27	28	20	
20	28	29	20	
20	29	30	21	
21	30	31	21	
21	31	32	22	

d. Loop construction listing

Figure 26. Concluded.

as shown in Fig. 26b. Each coordinate location should be numbered for ease in setting up the PFP model input deck. The coordinates of each point are then listed in numerical order as shown in Fig. 26c. Then the singularities (loops in most cases) are constructed by point number using the tabulation from Fig. 26b as shown in Fig. 26d. When listing the construction of a horseshoe vortex, it is necessary to start with a trail point and end with a trail point as shown in Fig. 1 of Vol. I. The singularity identification number indicates the type of singularity (1, indicates sources; 2, indicates loop vortices; 3, indicates trailing vortices). The routine in Section 5.0, Vol. I, or one similar to it, is then used to take the coordinates corresponding to the loop construction list, arrange in order, and convert the coordinates to the form necessary for input to the PFP. The routine also calculates the control point locations and unit velocity vectors in the manner of Section 3.3, Vol. I, as input to the PFP.

The typical layout and tabulation of an area where a wing attaches to a fuselage is shown in Fig. 27. The complex loop pattern shown in insert "A" was necessary to get the desired vortex spacing along the leading edge of the wing when it was modeled. The layout and tabulation of a section of the wing and pod are shown in Fig. 28. The shaded area is a separate wing part and is not included in the tabulation. An exploded view of the model by separate wing parts is shown in Fig. 29. (A second word of caution: where two wing parts join together, care should be taken to ensure that the common coordinates are identical.)

This configuration represents the largest model (1559 loop vortices and 20 horseshoe vortices, 1579 total) that has been run on the PFP. The analysis of this model is given in Section 4.3.

a. Line drawing layout

Fuselage (Continued)

Station → ㉒ ㉓ ㉓-1/2 ㉔ ㉕ ㉖ ㉗

x → n n n n n n n

Arrows show outline of wing part and triangular loop vortices. -A- See Fig 27a
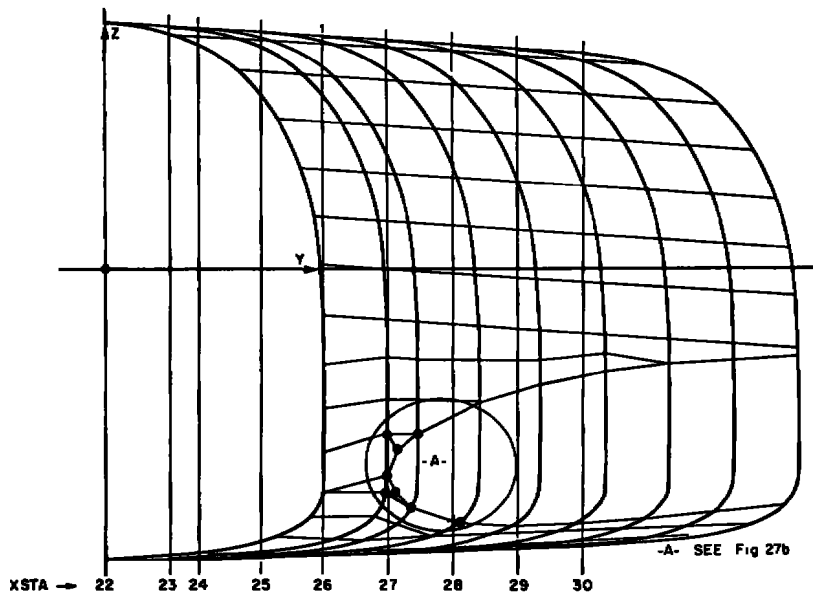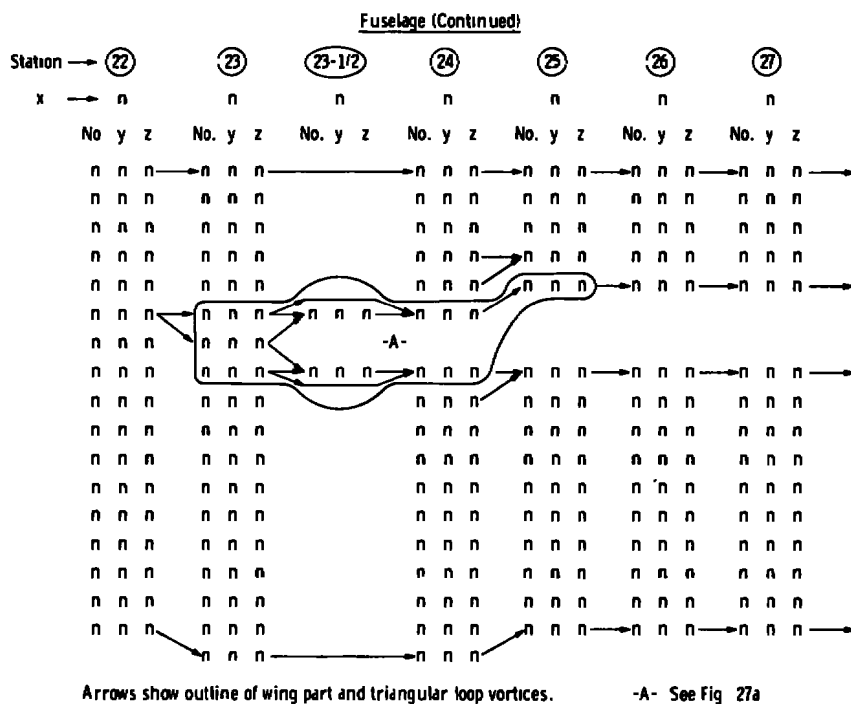
b. Coordinate tabulation method

Figure 27. Fuselage-wing junction for complex model.

a. Line drawing layout

Wing Bottom

Station →	①			②			③			④			⑤			⑥		
x →	n			n			n			n			n			n		
	No.	y	z	No.	y	z	No.	y	z	No.	y	z	No	y	z	No.	y	z
	n	n	n—→	n	n	n—→	n	n	n—→	n	n	n—→	n	n	n—→	n	n	n—→
	n	n	n	n	n	n	n	n	n	n	n	n	n	n	n	n	n	n
	·n	n	n	n	n	n	n	n	n	n	n	n	n	n	n	n	n	n
	n	n	n	n	n	n	n	n	n	n	n	n	n	n	n	n	n	n
	n	n	n	n	n	n	n	n	n	n	n	n	n	n	n	n	n	n
	n	n	n	n	n	n	n	n	n	n	n	n—→	n	n	n	n	n	n
	n	n	n	n	n	n	n	n	n	n	n	n	n	n	n	n	n	n
	n	n	n	n	n	n	n	n	n-	n	n	n	n	n	n	n	n	n
	n	n	n	n	n	n	n	n	n	n	n	n	n	n	n	n	n	n
	n	n	n	n	n	n	n	n	n	n	n	n	n	n	n	n	n	n
	n	n	n	n	n	n	n	n	n	n	n	n	n	n	n	n	n	n
	n	n	n	n	n	n	n	n	n	n	n	n	n	n	n—→	n	n	n—→
	n	n	n	n	n	n	n	n	n	n	n	n						
	n	n	n—→	n	n	n—→	n	n	n—→	n	n	n						

Arrows show outline of wing part and triangular loop vortices.

b. Coordinate tabulation method

Figure 28. Section of wing and pod for complex model.

Figure 29. Exploded view of complex model.

4.0 APPLICATION AND VERIFICATION

In the preceding discussions, the problem areas and potential solutions that are required to get an accurate simulation of an aerodynamic shape using a network of vortices were pointed out. The proof of the techniques used, of course, depends on modeling of actual vehicles which have had experiments conducted with them and com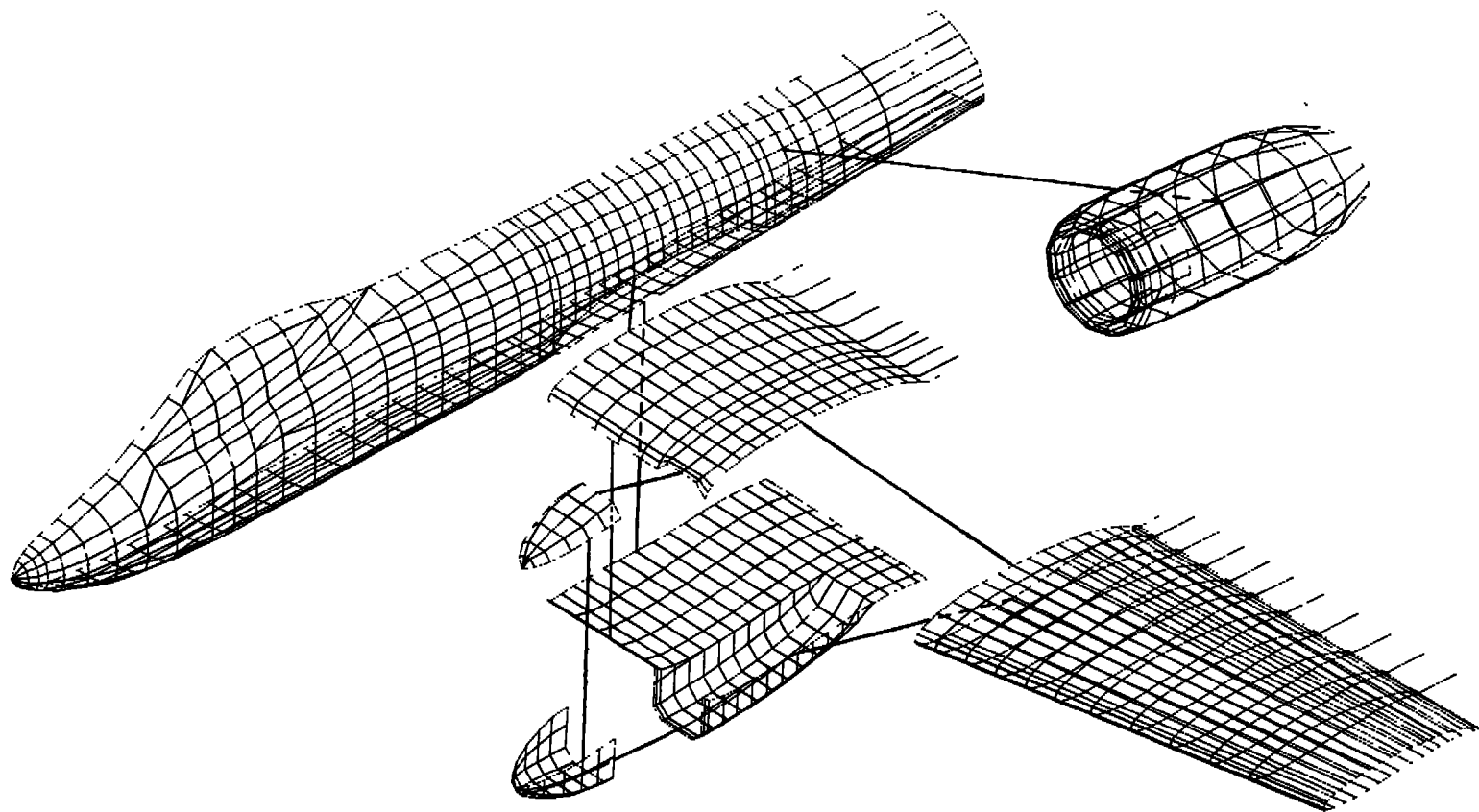paring theoretical flow field variables with those measured. The following sections describe a few practical applications of the PFP. In most cases, wind tunnel data are available to show the comparison of the theoretical predictions from the PFP with experimental data.

4.1 FUSELAGE MODEL

4.1.1 Inlet Flow Field Study

The fuselage model shown in Fig. 30 was used to verify the capabilities of the potential flow computer program. The objective of studying this configuration was to determine the flow field (upwash and sidewash) at the engine inlet fuselage location so that an effort could be made to duplicate the flow field by some type flow shaping device. Data were available from previous wind tunnel flow field studies at a Mach number of 0.9, which also allowed a check on the adequacy of correction used for compressibility in the PFP solutions. The complete plot of the math model and area location where the flow field was measured is shown in Fig. 31. The comparison between the predictions from the PFP and the wind tunnel data at a Mach number of 0.9 with a pitch angle of 25 deg is shown in Fig. 32. These data show excellent agreement.
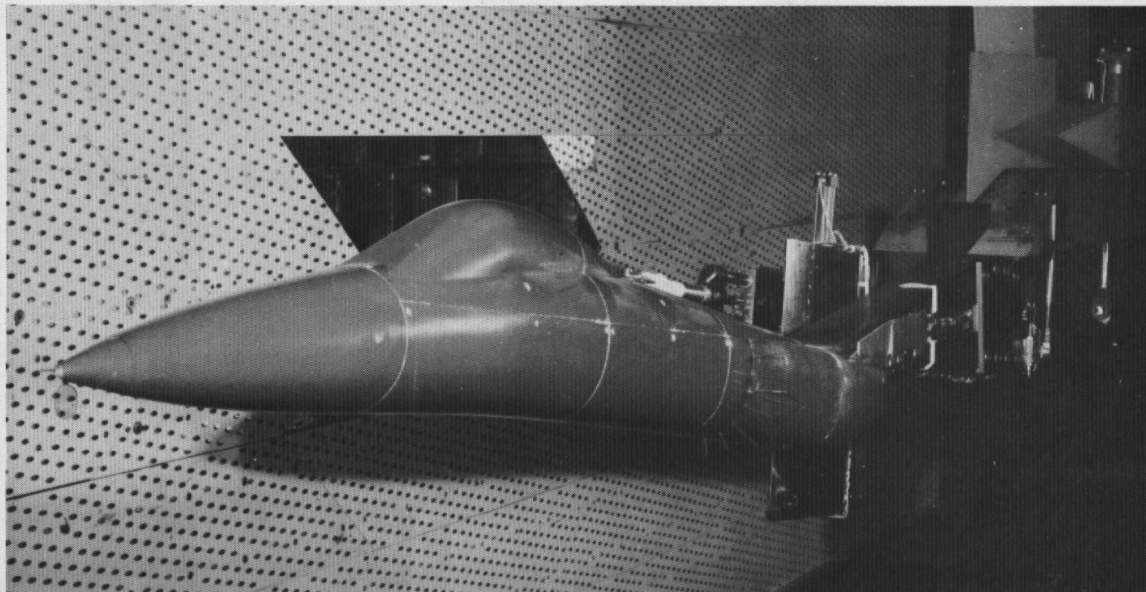

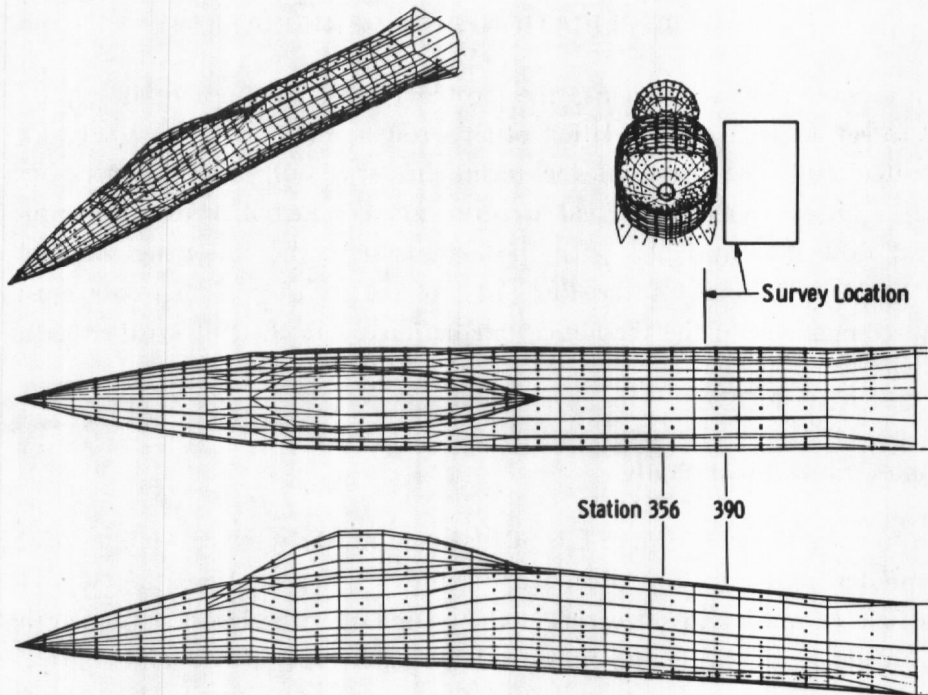Figure 30. Wind tunnel model of fuselage configuration.

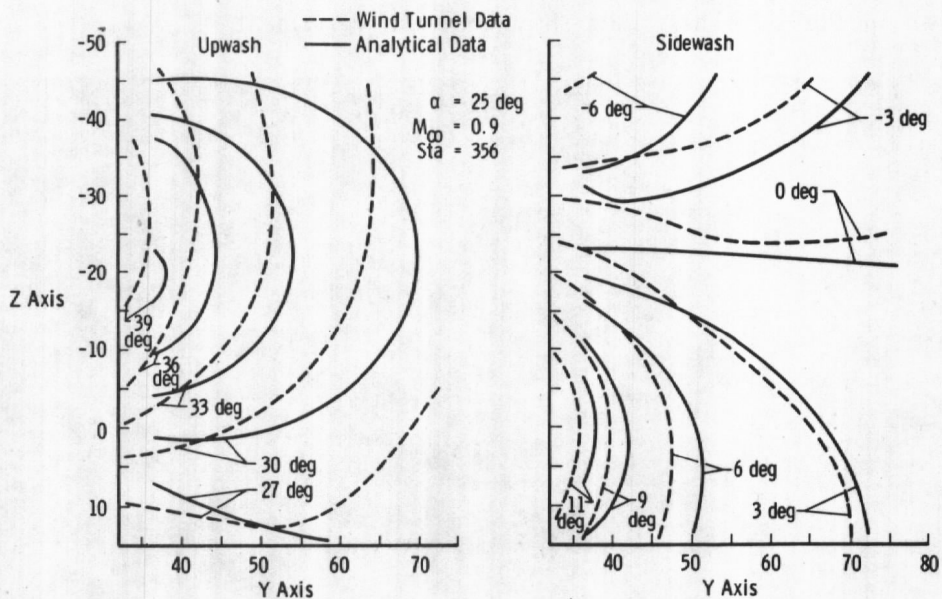Figure 31. Mathematical model of the fuselage configuration.

Figure 32. Comparison between analytical and wind tunnel data for
Mach number 0.9 at an angle of attack of 25 deg.

4.1.2 Missile Exhaust Ingestion Study

A study of missile exhaust ingestion was also made with this fuselage math model. For this study, the streamtube that enters the engine was needed. Since the path of the missile was known, it could be determined if the missile passed through the streamtube and for how long. The streamtube was determined by tracing streamlines from the four corners of the aircraft inlet upstream. By using the math model in Fig. 31 at low angles of attack, it was found that the problem shown in Fig. 10c occurred and additional circumferential rays had to be added as indicated by the dash lines in Fig. 33. This figure shows the streamtube for zero pitch angle at a Mach number of 0.9. The streamtubes for 25-deg angle of attack at a Mach number of 0.9 with two different inlet locations are shown in Fig. 34. At this angle of attack, the original math model was sufficient. Unfortunately, no experimental data exist to verify the accuracy of the streamtube location, but the data generated were very useful to estimate effects of missile gas ingestion on aircraft engine operation.
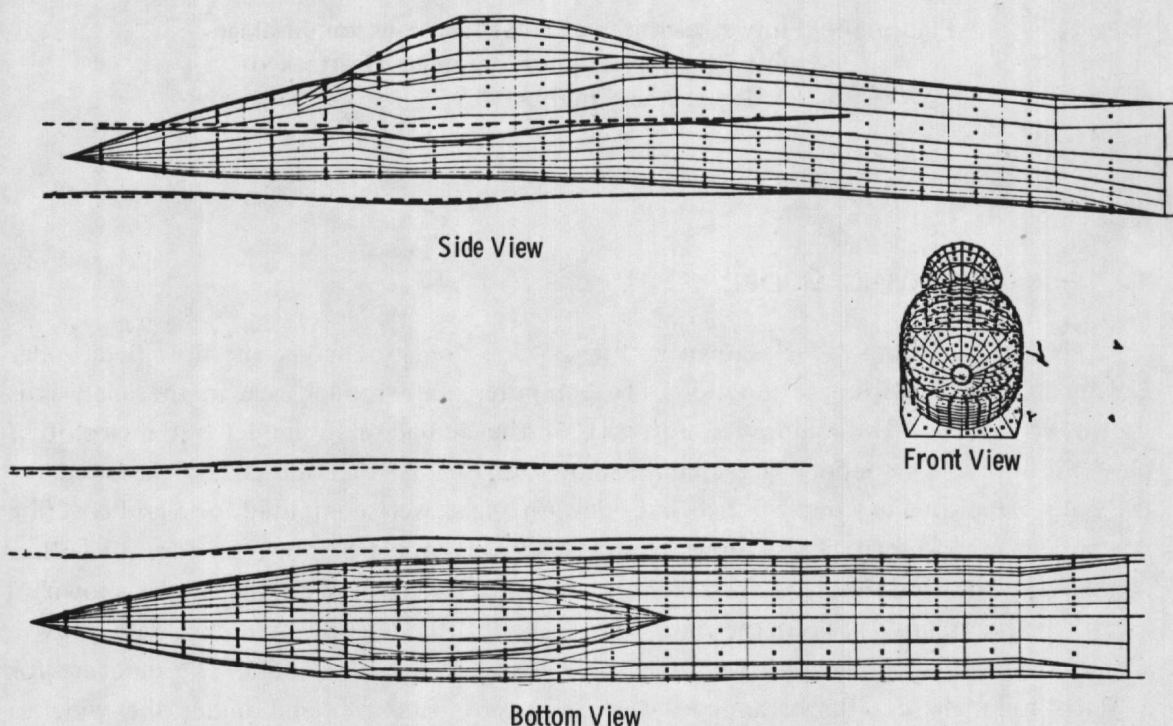

Side View

Front View

Bottom View

Figure 33. Flow streamtube to inlet location for fuselage model configuration at an angle of attack of zero at Mach number 0.9.
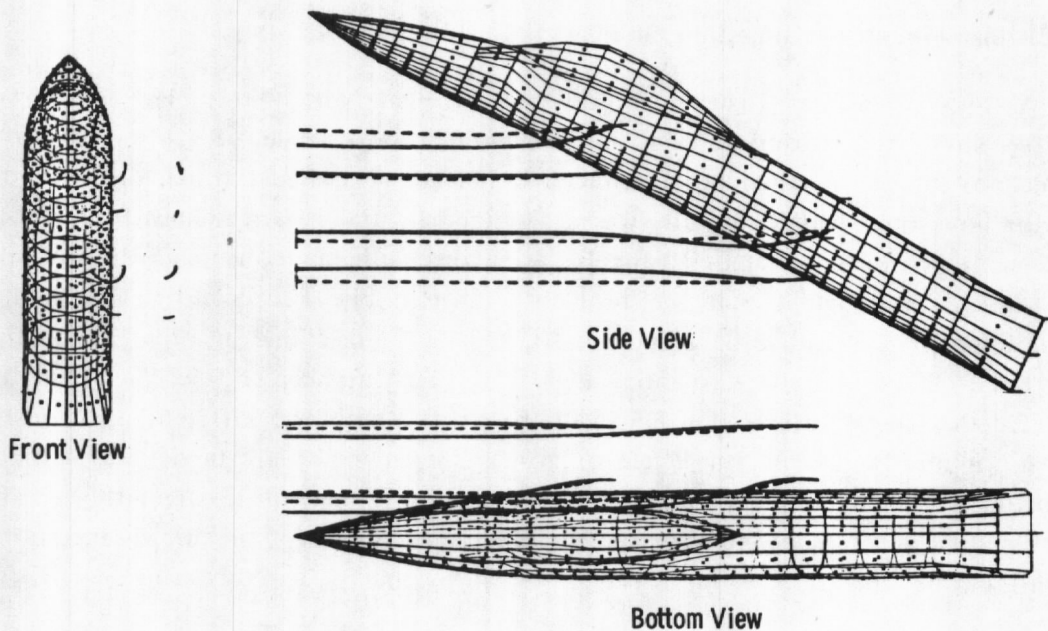
Figure 34. Flow streamtube to inlet locations for fuselage model configuration at an angle of attack of 25 deg at Mach number 0.9.

4.2 FUSELAGE-WING MODEL

The fuselage-wing model shown in Fig. 35 was used to analyze the flow field under a wing at the wing-fuselage junction. The computer math model used in the analysis is shown in Fig. 36. The canopy is not part of the actual math model but was plotted only for looks. The modeling technique shown in Fig. 20 (Section 3.2.3) was used for the outer panel of the wing. Upwash and sidewash angles were computed for a grid covering the survey area shown. These upwash and sidewash data are shown in Fig. 37 with a comparison to wind tunnel data taken at the same location with the model shown in Fig. 36. The trends between the data are excellent although the predicted data show a slightly higher gradient across the survey area than the measured data. The data are for a Mach number of 0.9. Streamlines were traced to pass over and under the wing to determine if any anomalies were present with this modeling technique. These streamlines are shown in Fig. 38 with no apparent problems indicated.
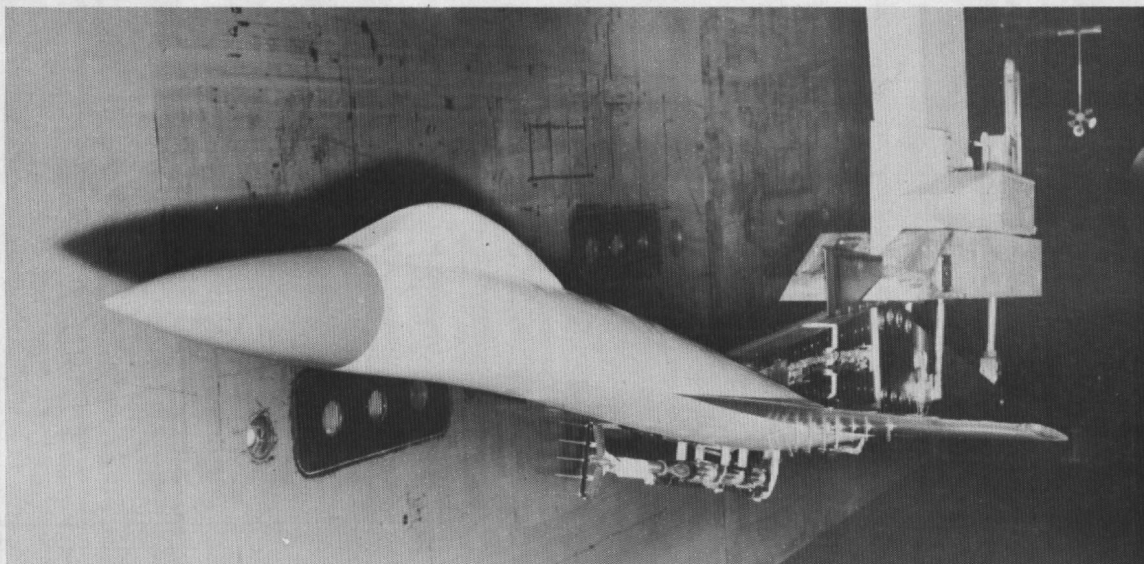
Figure 35. Wind tunnel model of fuselage-wing model.

Survey Location

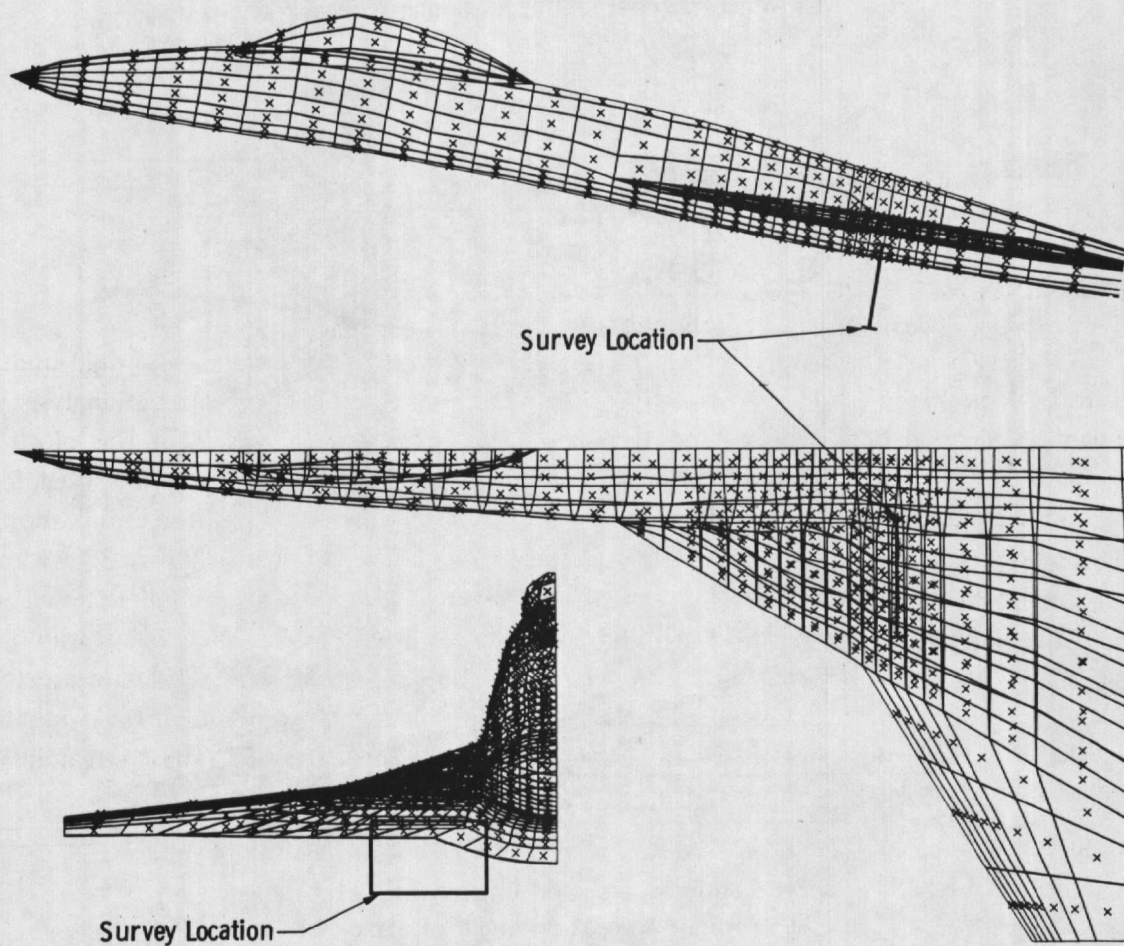Survey Location

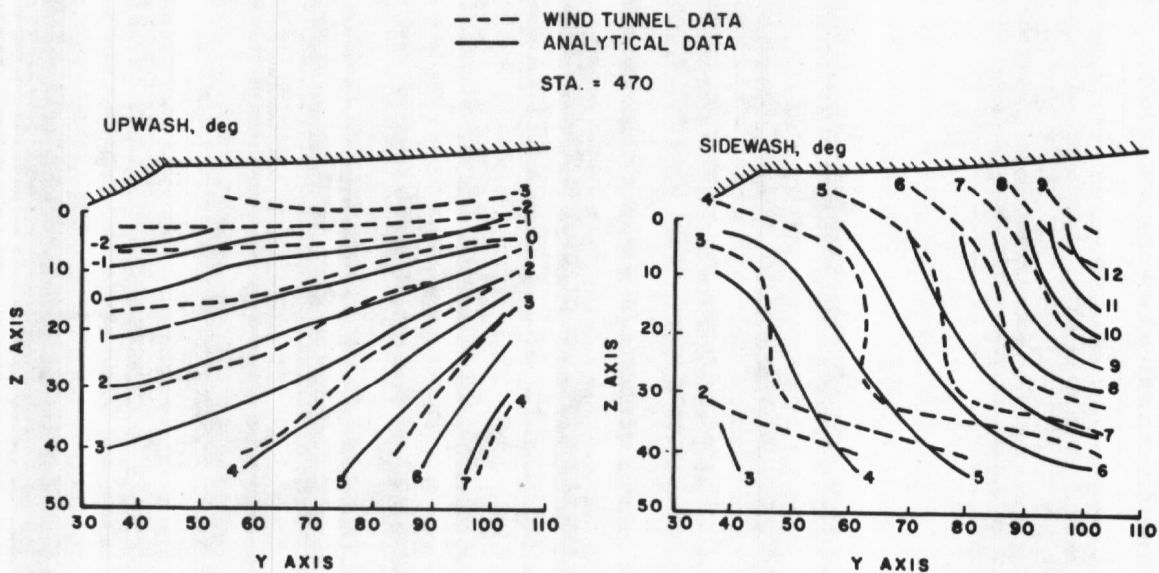Figure 36. Mathematical model of the fuselage-wing configuration.

Figure 37. Comparison between analytical and wind tunnel data
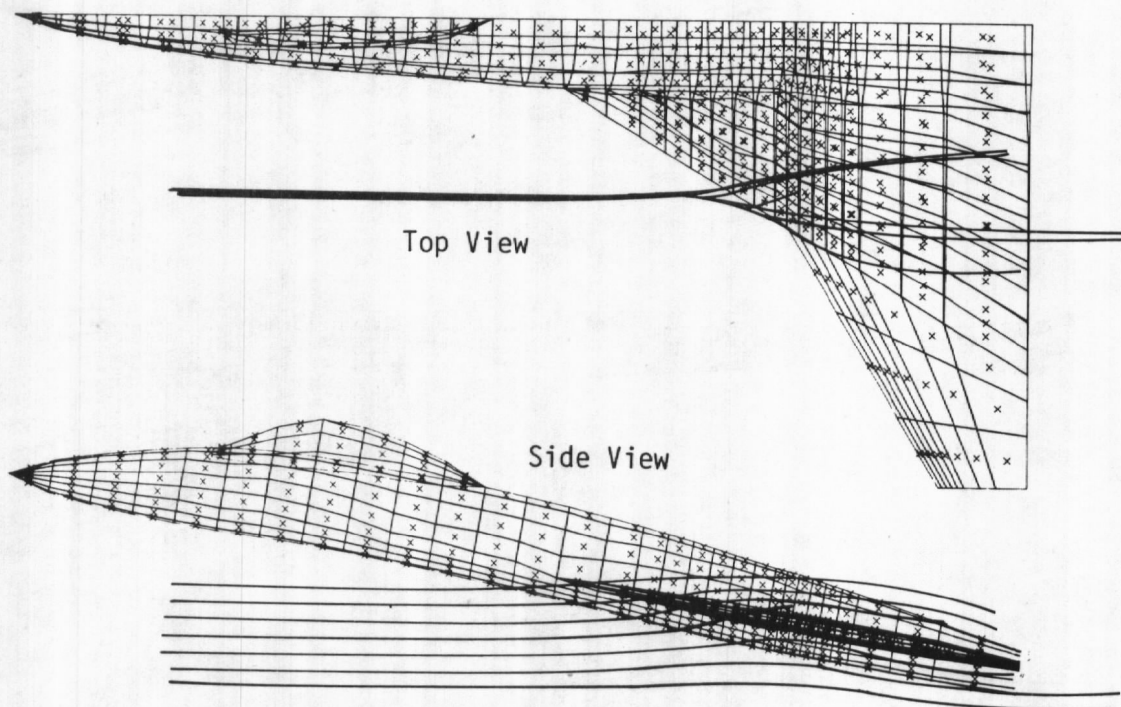for Mach number 0.9 at an angle of attack of 10 deg.

Figure 38. Flow streamlines over and under wing for fuselage-wing
model configuration at an angle of attack of 10 deg
at Mach number 0.9.

4.3 FUSELAGE-WING-NACELLE MODEL

The wind tunnel model shown in Fig. 39 was studied to determine the streamtube entering the engine for a configuration with the engine above and behind the wing. The math model of this configuration was used in Section 3.3 for the example of complicated modeling techniques. To verify the accuracy of the PFP solution, flow angularity data were taken at two points near the inlet during a CTS grid test in the AEDC 4-ft Aerodynamic Wind Tunnel (transonic, PWT-4T). Because the wind tunnel model had a flow-through inlet/nacelle, the math model was set up the same. However, the lip configuration of the math model was taken from production drawings and appeared to be slightly thicker than the wind tunnel model.

AEDC
73-1608

Figure 39. Wind tunnel model of fuselage-wing-nacelle model.

A comparison between the theoretical and experimental data is given in Fig. 40 and the data show excellent agreement. These data are for an 8-deg angle of attack at a Mach number of 0.3. The streamtube entering the inlet for this Mach number and angle of attack is shown in Fig. 41.

EXPERIMENTAL	THEORETICAL
$\epsilon = -6.15$ deg	$\epsilon = -6.54$ deg
$\sigma = 3.36$ deg	$\sigma = 3.38$ deg
$\epsilon = -13.47$ deg	$\epsilon = -13.43$ deg
$\sigma = 2.77$ deg	$\sigma = 5.46$ deg

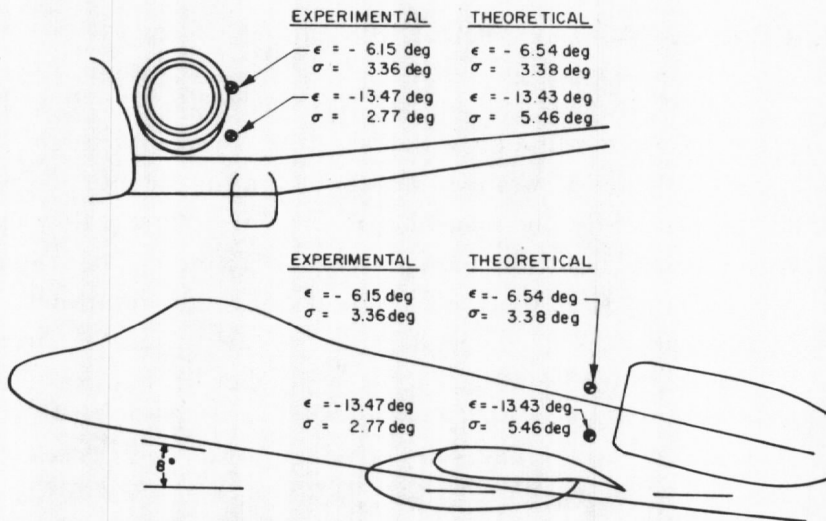| EXPERIMENTAL	THEORETICAL
$\epsilon = -6.15$ deg	$\epsilon = -6.54$ deg
$\sigma = 3.36$ deg	$\sigma = 3.38$ deg
$\epsilon = -13.47$ deg	$\epsilon = -13.43$ deg
$\sigma = 2.77$ deg	$\sigma = 5.46$ deg

Figure 40. Comparison between experimental and theoretical data for Mach number 0.3 at an angle of attack of 8 deg.
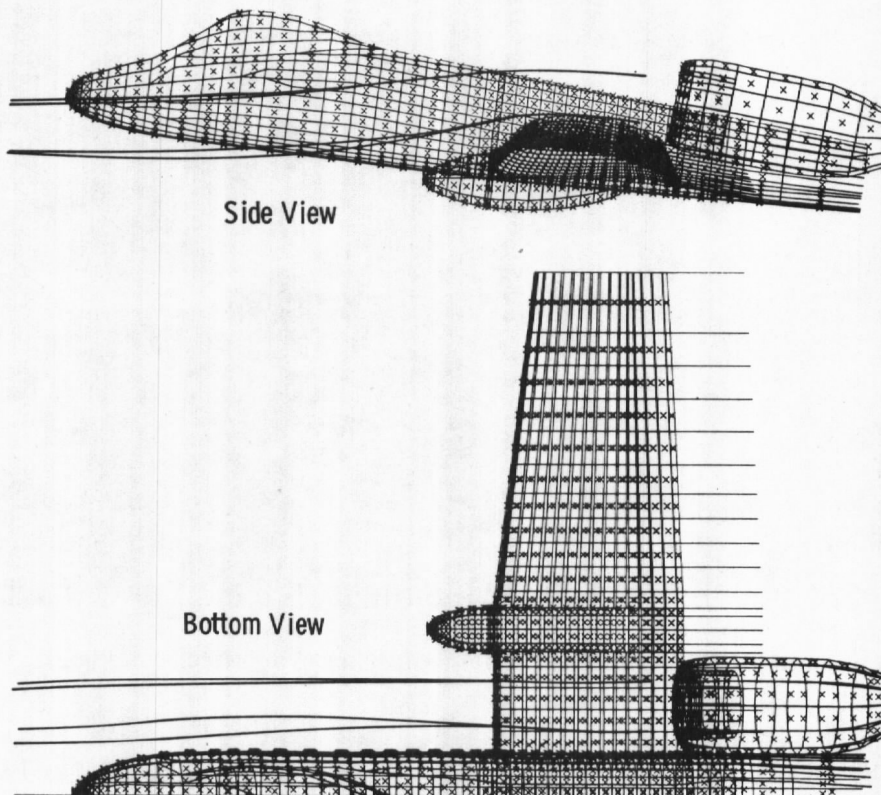

Side View

Bottom View

Figure 41. Flow streamtube entering the inlet at Mach number 0.3 at an angle of attack of 8 deg.

This particular analysis required very close modeling from the fuselage nose to the inlet and resulted in the largest model (1559 loop vortices and 20 horseshoe vortices) that has been run on the PFP. The computer time required for the analysis of one Mach number and model attitude was 16.5 hr on the AEDC IBM 370-155 which should reduce to approximately 4 hr on the new AEDC IBM 370-165.

4.4 CROSSWIND ANALYSIS MODEL

An analysis was made of an inlet/engine at takeoff power in a crosswind with the PFP. The analysis was made in support of a crosswind experiment conducted during an inlet study in the AEDC 16-ft Propulsion Wind Tunnel (transonic, 16T). The experiment simulated the aircraft at the end of the runway with takeoff power at zero forward velocity in crosswinds up to approximately 70 ft/sec. The crosswind was supplied by a 3-ft-diam simulator positioned perpendicular to the aircraft axis as shown in Fig. 42.
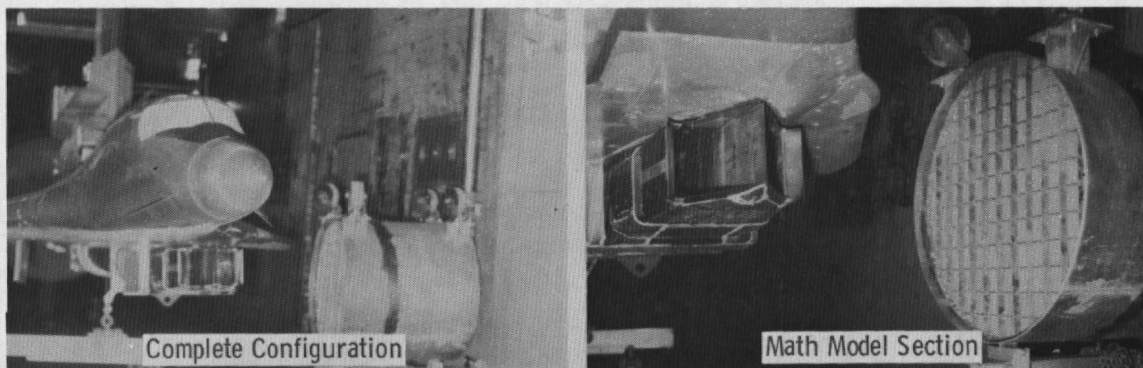

Complete Configuration

Math Model Section

Figure 42. Inlet test model and crosswind simulator.

The objective of the computer analysis was to determine if the 3-ft-diam crosswind simulator would adequately simulate the crosswind when used in conjunction with the inlet model and to determine the position for the simulator to give best results. The mathematical analysis was made with the inlet/engine in an infinite crosswind.

The math model included only a portion of the experimental model as shown in Fig. 43. The computer plot of the math model is shown in Fig. 44. This model included a simple inlet/engine and a segment of the wing. The engine ducts were closed at the downstream end, and a negative source was located near the rear center of each engine duct to produce the correct inlet mass flow when that particular engine was in operation. Streamlines were traced upstream from near the four corners of the inlet for each engine in operation to determine the flow pattern of the airstream entering the inlet.
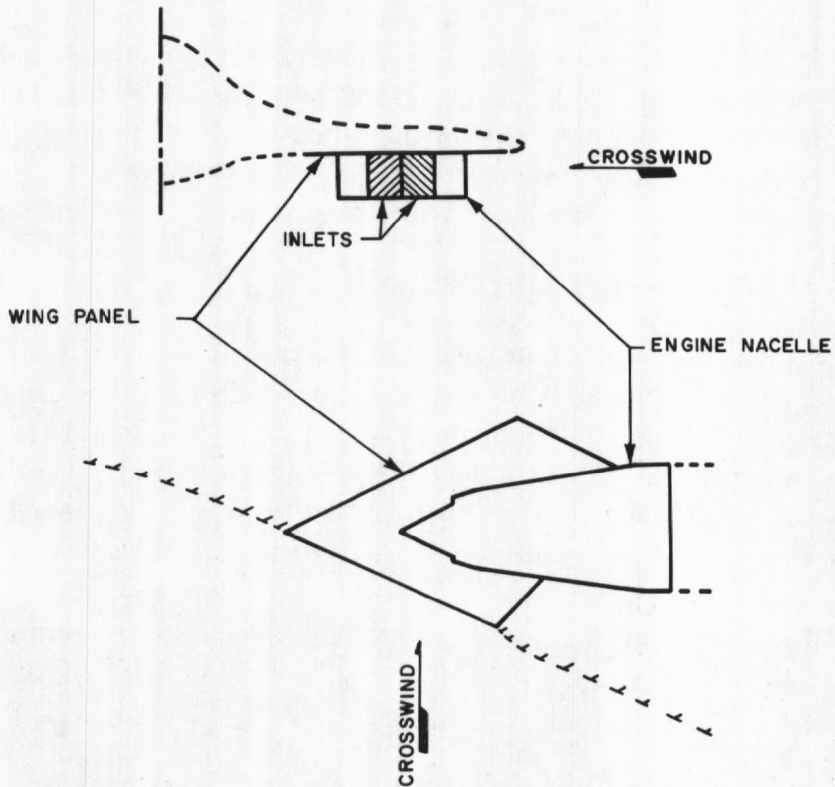
Figure 43. Sketch of the section of the test model duplicated with the mathematical model.
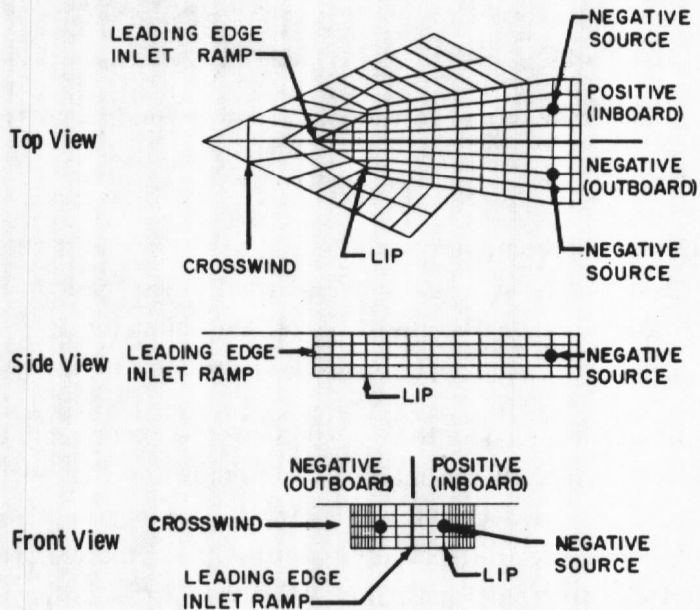

Figure 44. Basic mathematical model for the inlet/engine crosswind analysis.

Three different wing configurations were used to obtain the correct flow characteristics. The first configuration (Configuration 1, Fig. 45) was a minimum panel wing to use minimum computer time. This configuration was adequate for some of the test conditions; however, with a low crosswind velocity and the negative (outboard) engine off, the streamline from the top positive lip area passed over the wing. This was an impossible condition since the wing of the complete model actually covers this area. Therefore, a vortex sheet of trailing vortices was added (Configuration 2, Fig. 45) as a shield to block this flow path. This corrected the streamline characteristics for this test condition. However, with both engines on and a low crosswind velocity the vortex sheet of Configuration 2 had excessive leaks. Therefore, 22 additional panels plus the vortex sheet were added (Configuration 3, Fig. 45) to correct the streamline characteristics for this test condition. (Based on this analysis, it was found that when a solid surface is being simulated near an inlet where high mass flows are present the loop vortex panels should be extended out from the inlet at least three inlet diameters from the outside lip of the inlet to get correct simulation for all flow conditions. Configuration 1 was only slightly over 1 inlet diameter from the lip.)
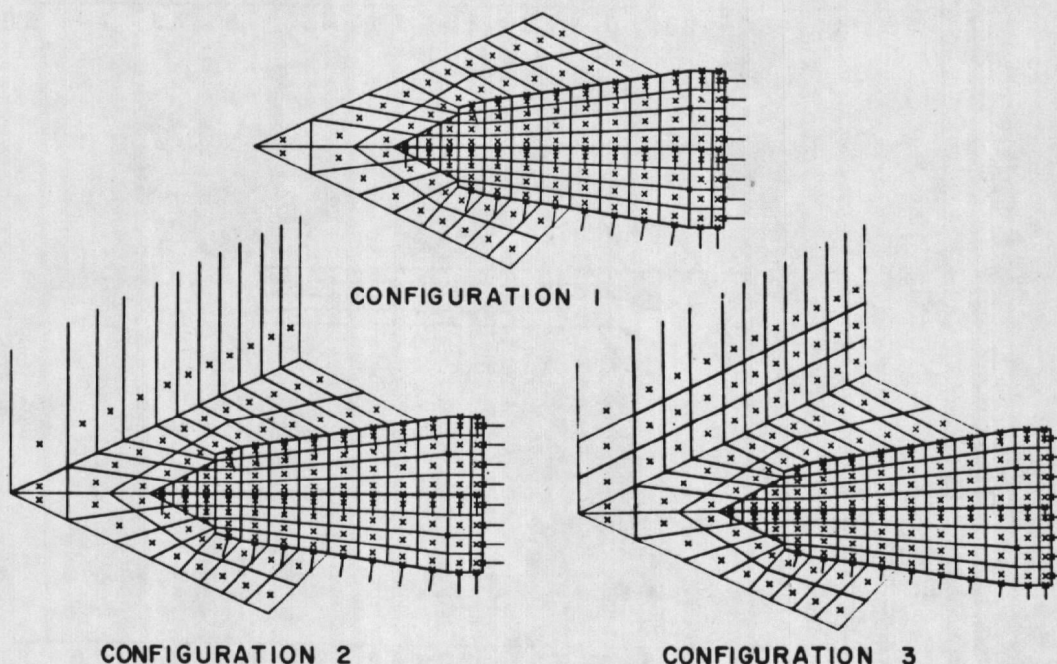
Figure 45. Mathematical models of wing configuration changes.

The flow streamlines for a typical engine mass flow/crosswind velocity combination are shown in Fig. 46. The recommended location of the simulator is shown on the figure. All of the streamlines originate within the area covered by the simulator. This indicates that the simulator should give a fair representation of the crosswind flow conditions and add a degree of confidence to the use of this crosswind simulation test.

Both Engines On

Mass Flow = 167.5 ft^3/sec per Engine

Crosswind Velocity = 67.5 ft/sec

Configuration 2

Simulator Position

a. Top view

Both Engines On

Mass Flow = 167.5 ft^3/sec per Engine

Crosswind Velocity = 67.5 ft/sec

Configuration 2

Simulator Position

b. Side view
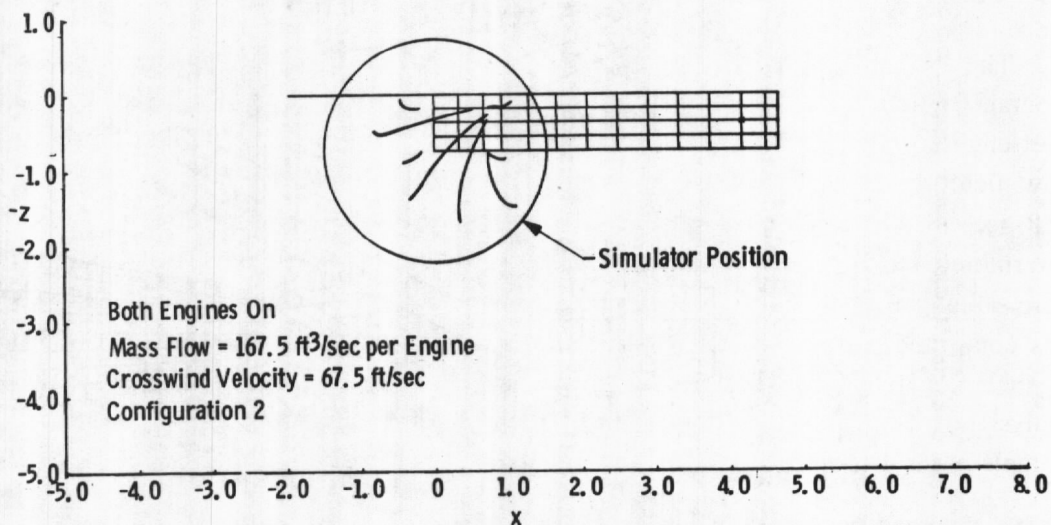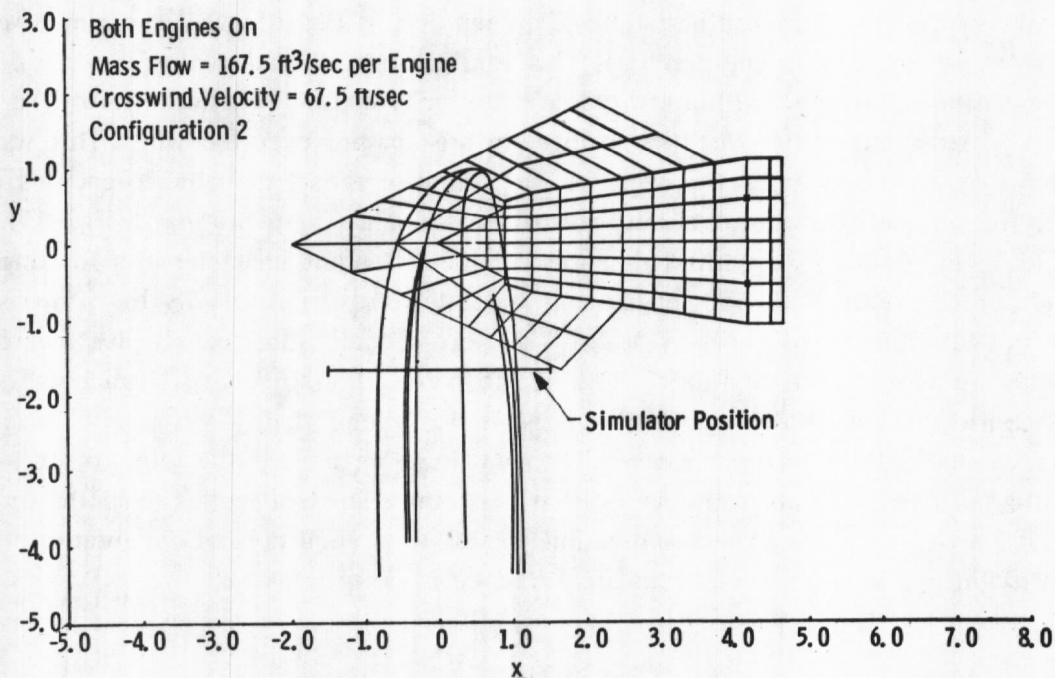
Figure 46. Flow streamlines for both engines on with a crosswind velocity of 67.5 ft/sec.

44

Both Engines On
Mass Flow = 167.5 ft³/sec per Engine
Crosswind Velocity = 67.5 ft/sec
Configuration 2

Simulator Position
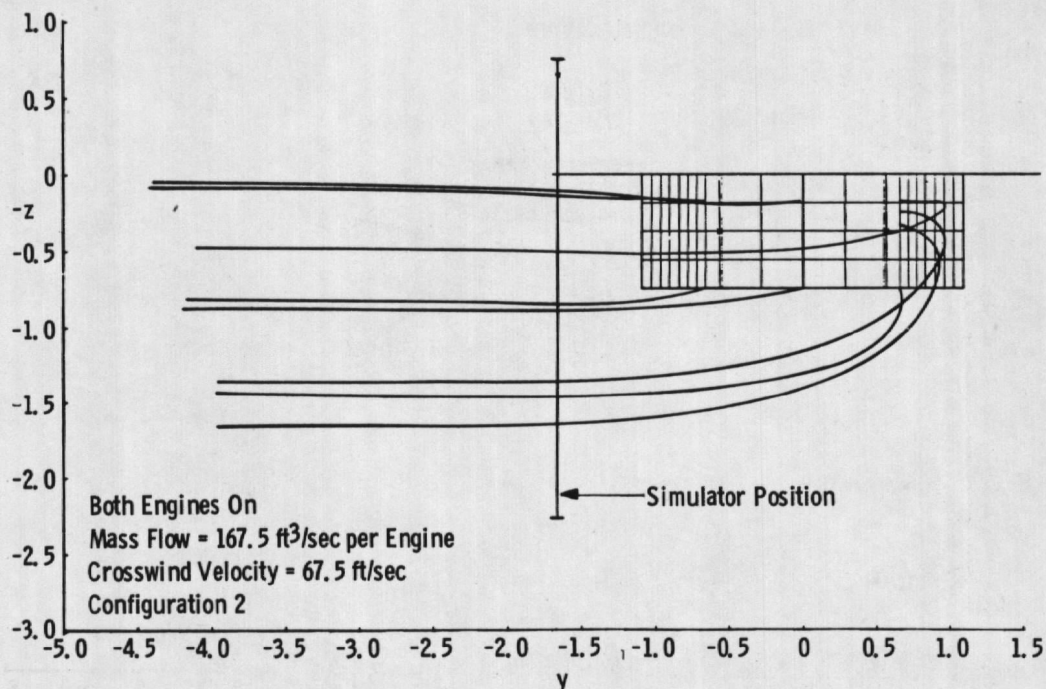
c. Front view
Figure 46. Concluded.

4.5 FLOW SHAPING DEVICES

The PFP in its present form was developed primarily to support an AEDC research program which had as an objective the development of a technique to test full-scale inlet/engine systems at high angles of attack and yaw. To accomplish this objective, the flow field about a typical highly maneuverable aircraft fuselage was analyzed using the PFP (see Section 4.1.1). Once the fuselage flow field at a typical inlet location was determined and the calculations verified by wind tunnel experiments, flow shaping devices were sought which could simulate the flow field at the inlet location. The flow field was computed, using the PFP, about various aerodynamic shapes which showed promise in their capability to simulate the desired inlet flow field. Some of the results of the analysis of two of these flow shaping devices are included in the next two sections. Complete results of the research program can be found in Refs. 1 and 2.

4.5.1 Dual Hollow Cylinders

The first shaping device analyzed that showed promise consisted of two hollow cylinders in proximity of each other. Unlike the previous models discussed which were fabricated and in all but one case (Crosswind Analysis Model, Section 4.4) were wind tunnel tested prior to the PFP analysis, the cylinder design shape and spacing were determined from the PFP analysis, and then the model was fabricated and wind tunnel tested. The mathematical model of the cylinders is shown in Fig. 47. The last
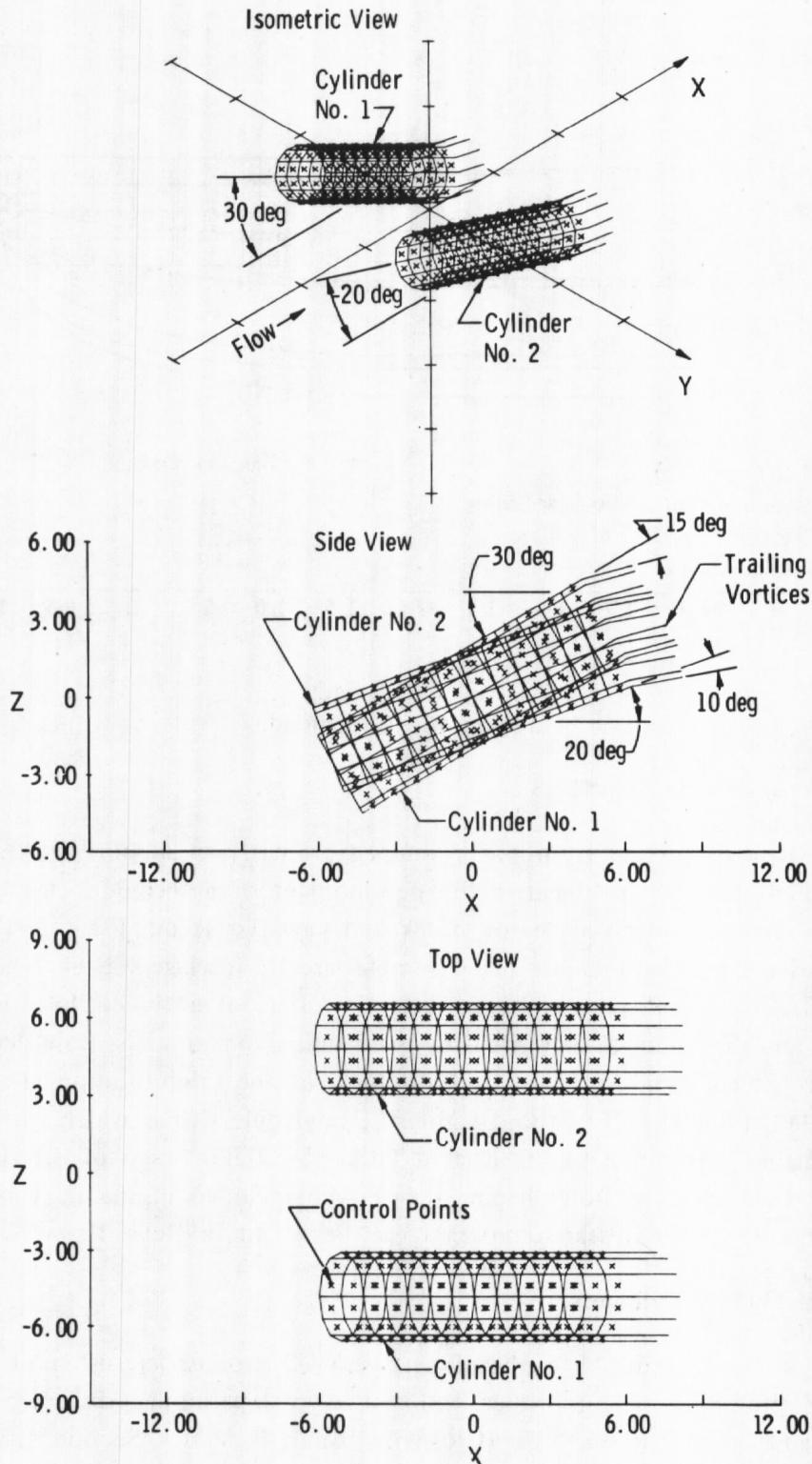
45

Figure 47. Mathematical model of the dual hollow circular cylinder configuration.

circumferential ray on each cylinder had trailing vortices. These were trailed at an angle equal to one-half the cylinder pitch angle. The object of this type device was to deflect the flow upward as it passed between the inclined cylinders. The wind tunnel models of the dual cylinders are shown in Fig. 48. A comparison between the theoretical and experimental flow angularity data is shown in Fig. 49. The lines are for constant theoretical flow angle (both upwash and sidewash) and the solid symbols show the location of the experimental data with the magnitude of the measured angles as indicated. The Mach number for these data was 0.9. The PFP overestimated the flow inclination angles by approximately 1 deg.
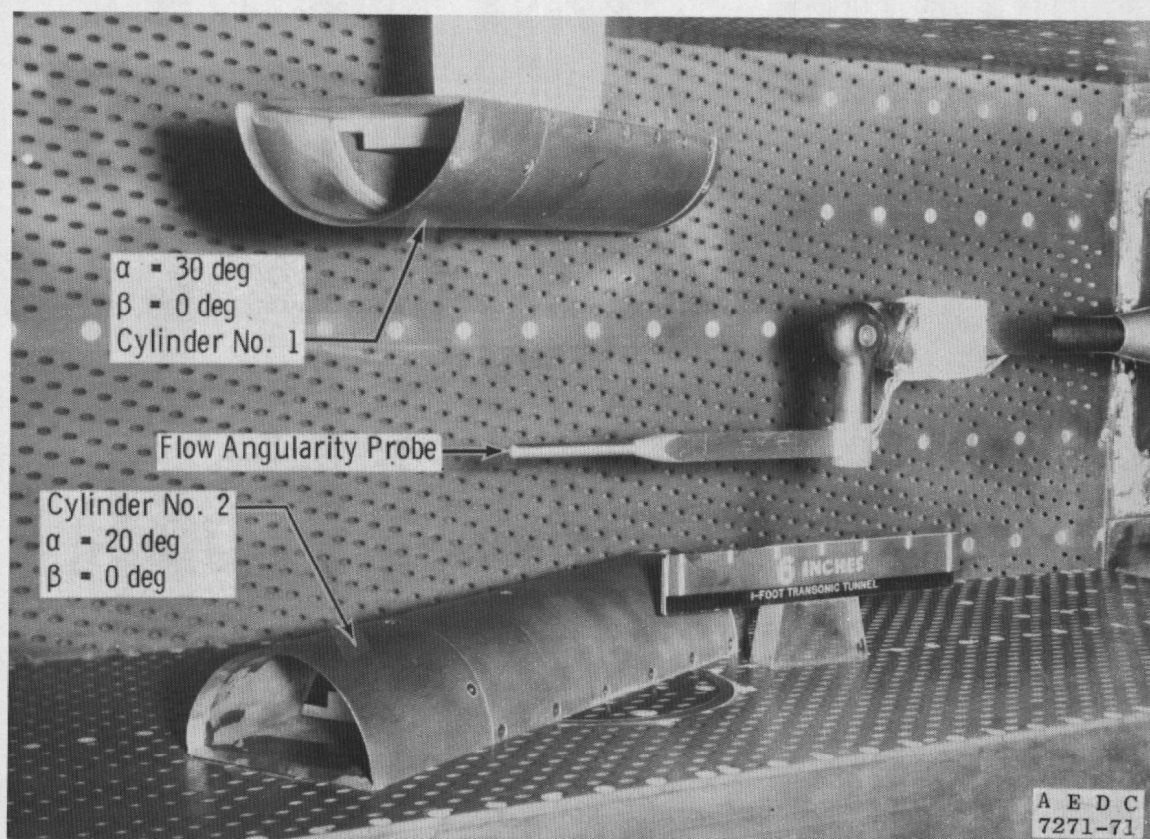

Figure 48. Dual hollow cylinders installed in the AEDC 1-ft transonic wind tunnel.

4.5.2 Turning Vanes

Another flow shaping device that was analyzed consisted of two turning vanes in proximity to each other. The mathematical model of this device is shown in Fig. 50. The vanes were modeled as two vortex sheets with the vortices trailed at one-half the angle between a line tangent to the trailing edge and the free stream. The wind tunnel
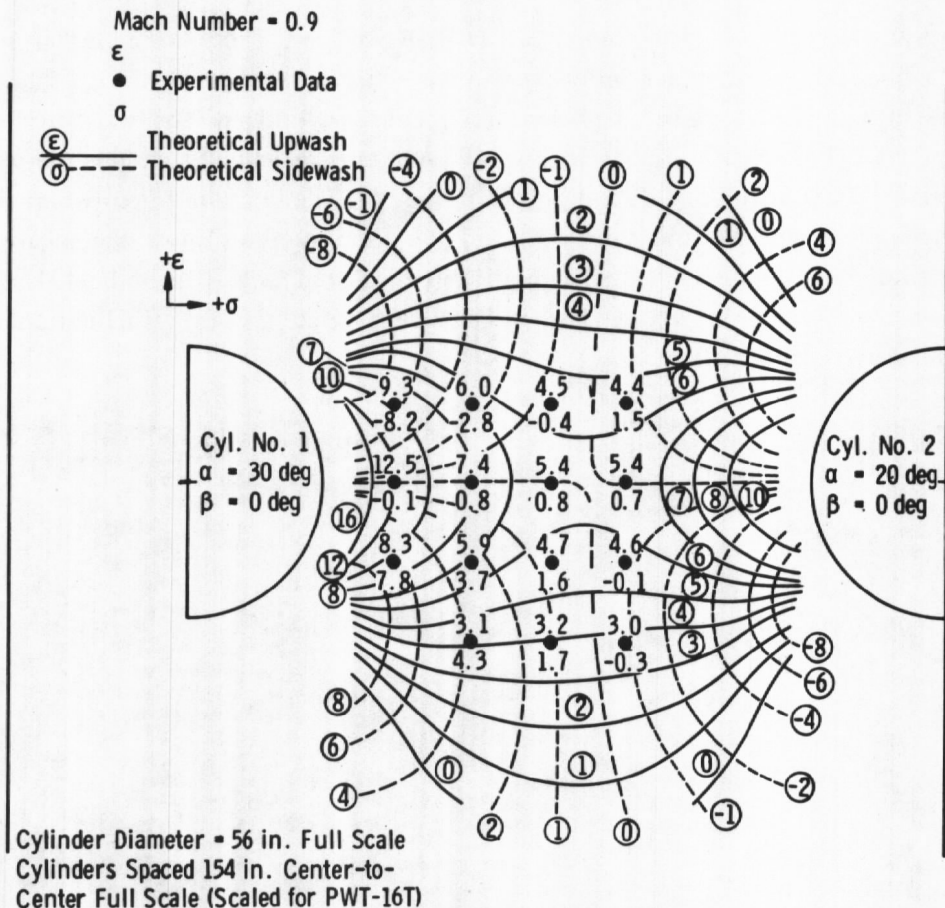
47

Figure 49. Experimental and theoretical comparison of upwash and sidewash angles for the dual hollow circular cylinders at a Mach number of 0.9.

models of the vanes are shown in Fig. 51. A comparison between the experimental data and theoretical data obtained with this math model is shown in Fig. 52. Again the lines represent constant theoretical flow angles, and the solid symbols represent the location of the experimental data with the magnitude as shown. The data are for a Mach number of 0.9. The experimental and theoretical data have the same trends; however, the magnitudes differ by 3 or 4 deg. Examination of the wind tunnel models in Fig. 51 shows that Vane No. 2 resembles an airfoil and the use of normal lifting surface modeling techniques was sufficient. However, Vane No. 1 has a very blunt trailing edge that, no doubt, caused flow separation and a low-pressure region resulting in a flow around the trailing edge of the vane rather than the outflow indicated by the theoretical data. In an attempt to get better simulation of the actual wind tunnel model, the math model was modified to trail the vortices of Vane No. 1 at a minus 10 deg as shown in Fig. 53. This modification decreased the theoretical data by approximately 1 deg as shown in Fig. 54 and brought the difference in magnitude between the data to 2 or 3 deg.
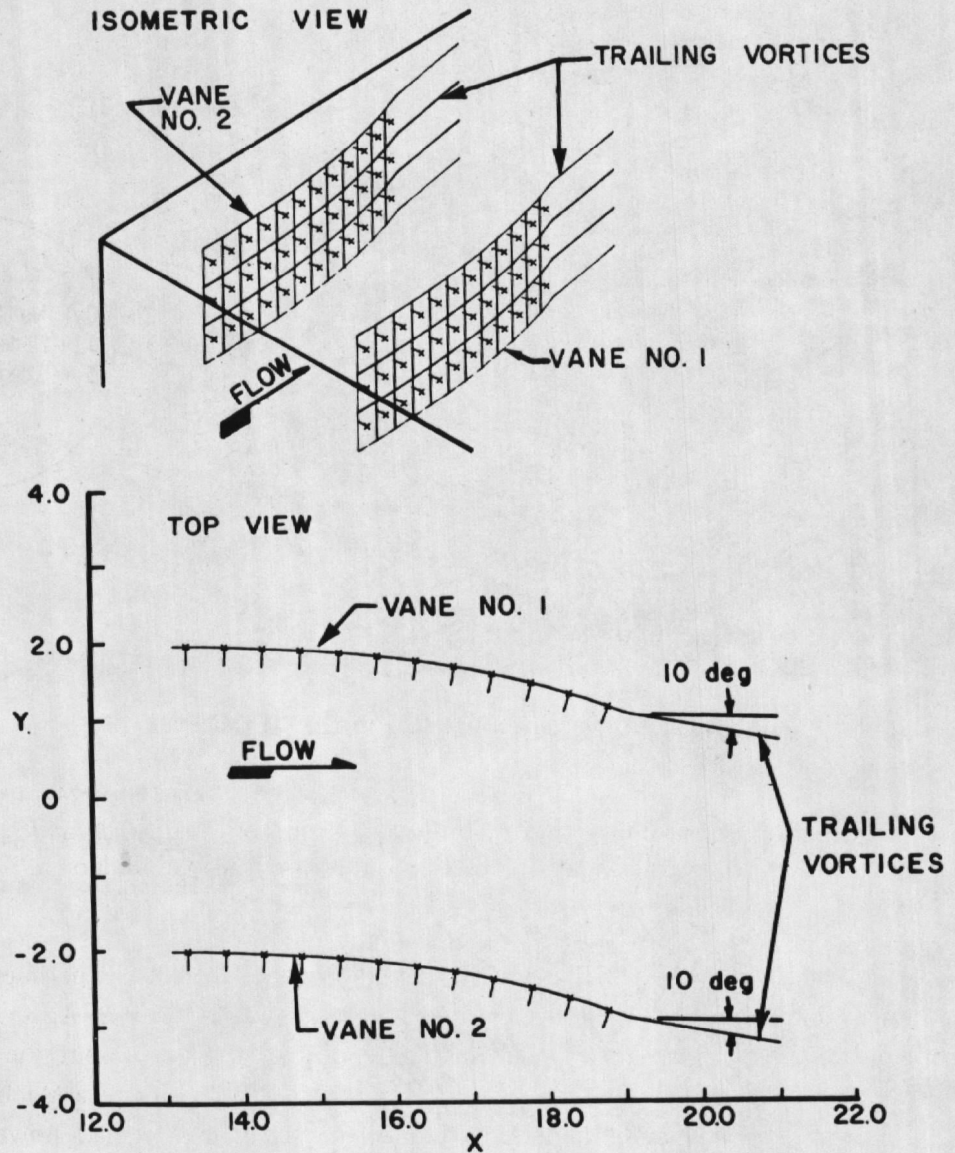
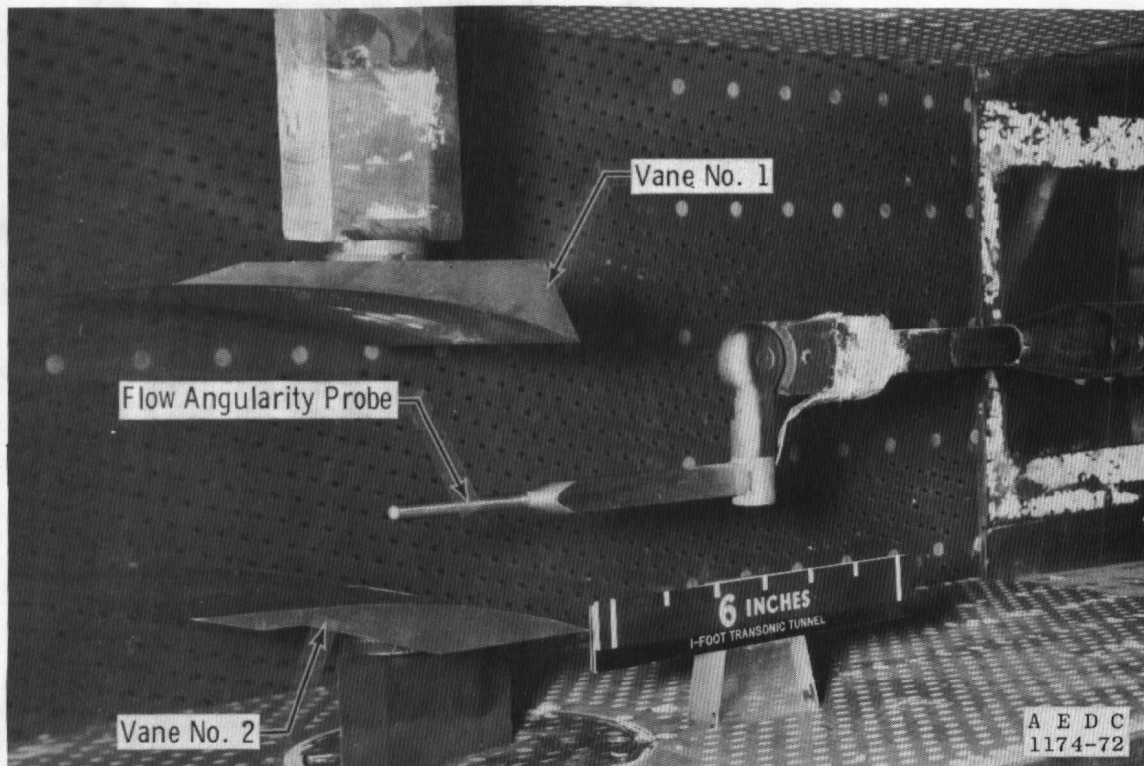Figure 50. Mathematical model of the turning vanes.

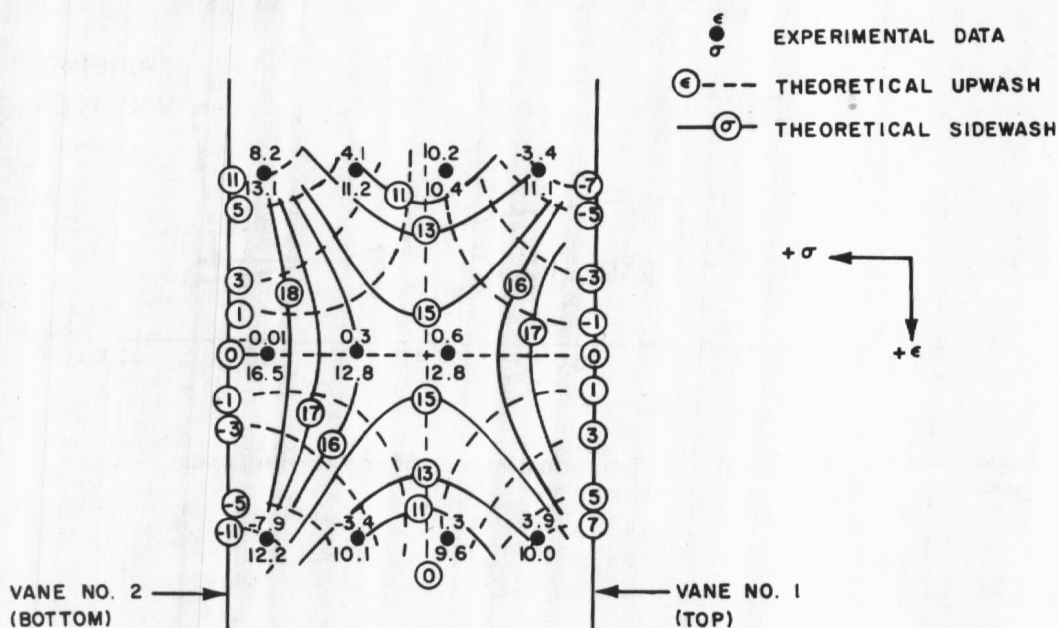Figure 51. Turning vanes installed in the AEDC PWT-1T.

Figure 52. Comparison between experimental and theoretical data
for turning vanes at a Mach number of 0.9 with 10-deg
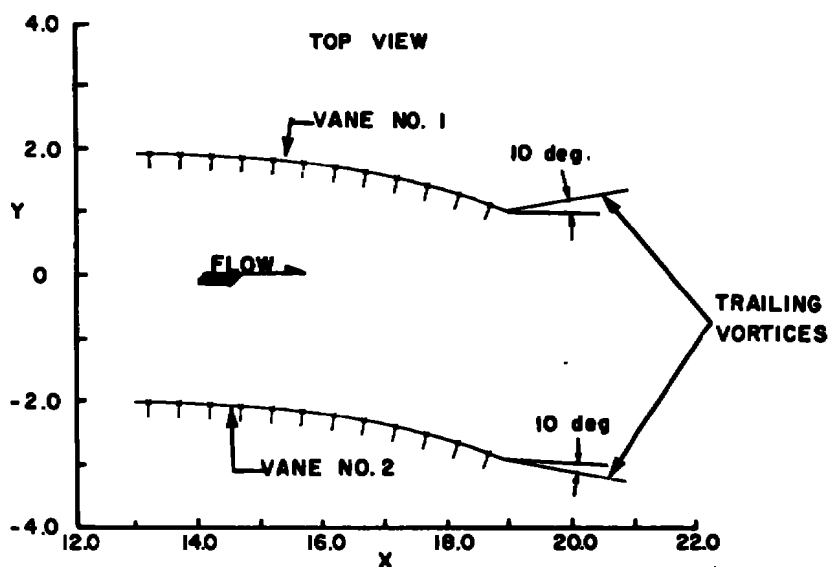trailing vortices from both vanes.

Figure 53. Mathematical model of the turning vanes with modified
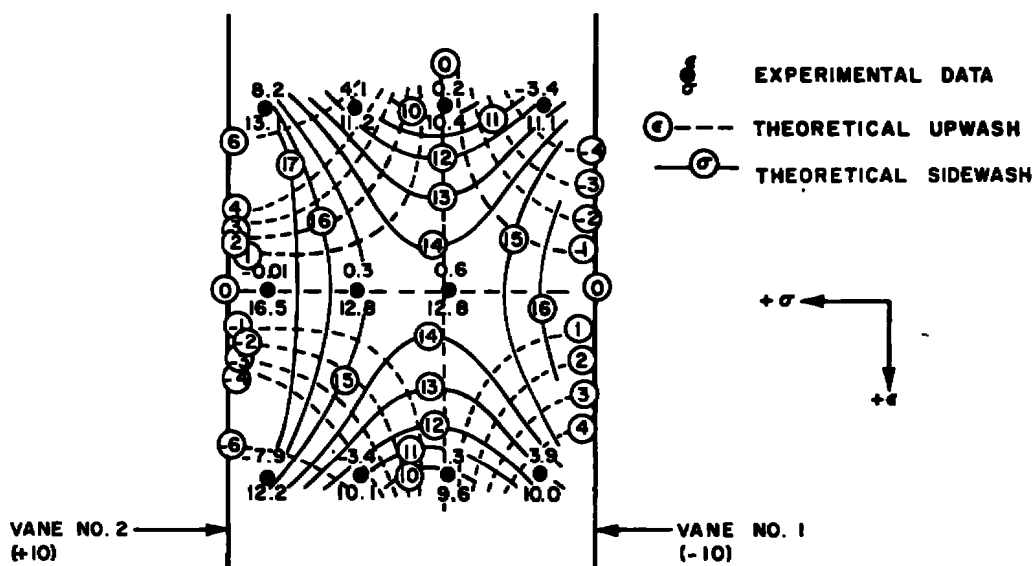trailing vortices from vane No. 1.

Figure 54. Comparison between experimental and theoretical data
for turning vanes at a Mach number of 0.9 with the
trailing vortices from vane No. 1 modified to trail
at -10 deg.

5.0 CONCLUDING REMARKS

This volume has outlined the types of data available using the AEDC PFP and has attempted to give the reader a better than average knowledge of the techniques and problems involved in setting up the mathematical models for the program. The techniques and problems discussed are ones that have been used or encountered during development and use of the program at AEDC. There has been no effort to cover all possible problems since each model is to some degree unique. The report does, however, verify the accuracy of the PFP for predicting flow fields around both simple and complex model configurations over a Mach number range from 0 to 0.9. The report has also demonstrated the PFP to be a useful tool in aircraft development and wind tunnel testing.

REFERENCES

1. Palko, R. L. "Full-Scale Inlet/Engine Testing at High Maneuvering Angles at Transonic Velocities." AIAA Paper No. 72-1026, Presented at the AIAA Seventh Aerodynamic Testing Conference, Palo Alto, California, September 13-15, 1972.

2. Palko, R. L. "A Method to Increase the Full-Scale Inlet/Engine System Testing Capability of the AEDC 16-Ft Transonic Wind Tunnel." AEDC-TR-73-9 (AD762912), June 1973.

3. Rubbert, P. E. "Theoretical Characteristics of Arbitrary Wings by a Non-Planar Vortex-Lattice Method." Boeing Company Document D6-9244, The Boeing Company, Seattle, Washington, August 1962.

4. Heltsley, F. L. and Parker, R. L., Jr. "Application of the Vortex-Lattice Method to Represent a Jet Exhausting from a Flat Plate into a Crossflowing Stream." AEDC-TR-73-57 (AD762502), June 1973.

5. Parker, R. L., Jr. and Heltsley, F. L. "Simulation of a High Disc Loading Free Propeller in a Cross Flow by the Vortex-Lattice Method." AEDC-TR-72-139 (AD751463), November 1972.

NOMENCLATURE

BL   Butt line

C_p Pressure coefficient

CTS   Captive trajectory system

c   Chord ·

HRL   Horizontal reference line

M_∞ Free-stream Mach number

n   Coordinate numerical value

S   Span

Sta   Station

WL   Waterline

x   Coordinate along tunnel axis, positive downstream

y   Horizontal coordinate, sign as indicated

z   Vertical coordinate, sign as indicated

a Model angle of attack, deg, positive up

β Model angle of yaw, deg, sign as indicated

ϵ Upwash, deg, positive up

θ Angle between wing mean line and free-stream velocity vector

σ Sidewash, deg, positive as indicated